

Cinnamyl alcohol dehydrogenases in the mesocarp of ripening fruit of *Prunus persica* genotypes with different flesh characteristics: changes in activity and protein and transcript levels

Damiano Gabotti, Noemi Negrini, Silvia Morgutti*, Fabio F. Nocito and Maurizio Cocucci

Department of Agricultural and Environmental Sciences - Production, Landscape, Agroenergy,
University of Milan, 20133 Milan, Italy

*Corresponding author: Silvia Morgutti

e-mail: silvia.morgutti@unimi.it

Abstract

Development of fruit flesh texture quality traits may involve the metabolism of phenolic compounds. This study presents molecular and biochemical results on the possible role played by cinnamyl alcohol dehydrogenase (CAD; EC 1.1.1.195) during ripening [S3, S4 I (pre-climacteric) and S4 III (climacteric) stages] of peach [*Prunus persica* (L.) Batsch] fruit with different flesh firmness (NMF ‘Oro A’/MF ‘Springcrest’ and ‘Sanguinella’) and colour (blood-flesh ‘Sanguinella’). Twenty-four putative full-length *PRUPE_CAD* genes were identified (in silico analysis) in the Peach Genome. The most abundant CAD isoforms, encoded by genes located on scaffolds 8 and 6, were probed by specifically developed anti-*PRUPE_CAD* sc8 and by anti-FaCAD (*PRUPE_CAD* sc6) polyclonal antibodies, respectively. *PRUPE_CAD* sc8 proteins (SDS- and native-PAGE/Western blot) seemed responsible for the CAD activity (in vitro/in gel assays) that increased with ripening (parallel to *PRUPE_ACO1* transcripts accumulation and ethylene evolution) only in the mesocarp of ‘Oro A’ and blood-flesh ‘Sanguinella’. Accumulation of *PRUPE_CAD* sc8 transcripts (qRT-PCR) occurred in all three cultivars, but in ‘Oro A’ and ‘Springcrest’ it was not always accompanied by that of the related proteins suggesting possible post-transcriptional regulation. Flesh firmness, as well as levels of lignin, total phenolics and, where present (‘Sanguinella’), anthocyanins, declined with ripening, suggesting that, at least in the studied peach cultivars, CAD activity is related to neither lignification nor differences in flesh firmness (NMF/MF). Further studies are necessary to clarify whether the high levels of CAD activity/expression in ‘Sanguinella’ play a role in determining the characteristics of this blood-flesh fruit.

Abbreviations

Abs, absorbance;
APS, ammonium persulfate;
BSA, bovine serum albumine;
CAD, cinnamyl alcohol dehydrogenase;
CCR, cinnamoyl CoA reductase;
CTAB, cetyltrimethylammonium bromide;
DAFB, days after full bloom;
DEPC, diethylpyrocarbonate.
DTT, dithiothreitol;
EU, enzyme units;
KLH, keyhole limpet hemocyanin;
 β -MSH, β -mercaptoethanol;
PAGE, polyacrylamide gel electrophoresis;
PMSF, phenyl-methyl-sulfonyl-fluoride;
PRUPE, *Prunus persica*;
PVPP, polyvinylpolypyrrolidone;
REF1, Reduced Epidermal Fluorescence;
RT, room temperature;
TBS-T, tris buffered saline-tween buffer;
TEMED, N,N,N',N'-tetramethylethylenediamine;
Tris, tris(hydroxymethyl)aminomethane

Introduction

Fruit breeding has traditionally privileged traits connected to fruit size and appearance, with organoleptic and nutritional properties remaining secondary goals (Monet and Bassi 2008). Nevertheless, nowadays consumers realize the connection between diet and health and therefore much more attention is given to the possibility of associating diet with prevention of a number of chronic-degenerative diseases (Sloan 2008). Fruits and vegetables are rich in antioxidant and nutritional molecules produced by secondary metabolism, with particular regard to phenolic compounds. Fruits with higher phenolic contents generally show stronger antioxidant properties (Lima et al. 2014). Anthocyanins, the coloured natural compounds widely distributed in fruits and vegetables, confer bright attractive red-purple colours to plant-derived foods; they are important determinants of their sensory and nutritional qualities (Tomás-Barberan et al. 2000) and also possess notable anti-inflammatory and antioxidant activity providing substantial health benefits to the diet (de Pascual-Teresa 2014, Vauzour et al. 2010 and references therein).

Flesh texture, highly dependent on the physico-chemical properties of the fruit cell walls, is an important determinant of fruit quality (Bassi and Monet 2008). Typical of fruit ripening is softening, mainly ascribable to the dissolution of the middle-lamellar pectic polysaccharides involved in cell adhesion. This phenomenon has deep effects on mesocarp tissue that progressively loses the stiffness of the juvenile phases to become soft and squishy. In peach (*Prunus persica* (L.) Batsch) fruit, evidences regarding different flesh firmness phenotypes, i.e., Melting Flesh (MF), Non Melting Flesh (NMF), Slow Melting Flesh and Stony Hard, indicate that the *endo-PG* gene and its protein product, endo-PG, are key factors in the determination of this trait (Ghiani et al. 2011, Lester et al. 1996, Morgutti et al. 2006, Peace et al. 2005), although other proteins, such as expansins, also play an important role in the determination of flesh texture (Hayama et al. 2003).

Fruit flesh texture is also affected by polyphenols acting at the cell wall level. Lignification processes in loquat (*Eriobotrya japonica*; Cai et al. 2006a, 2006b, Shan et al. 2008) and mangosteen (*Garcinia mangostana*; Dangcham and Ketsa 2007, Dangcham et al. 2008) fruits result in greater flesh firmness, toughness of the texture or loss of juiciness. Changes in the expression/activity/balance of the main enzymes involved in lignin biosynthesis may affect fruit flesh texture. The expression of cinnamyl alcohol dehydrogenase (CAD; EC 1.1.1.195), which catalyzes the reduction of cinnamaldehydes to cinnamyl alcohols conditioning the availability of monolignols, precursors in lignin biosynthesis (Mansell et al. 1974), is higher in firmest fruits of loquat (Shan et al. 2008) and strawberry (Salentijn et al. 2003). CAD-deficiency may induce the production of lignin richer in aldehydes and more susceptible to degradation, leading to development of softer fruit (Salentijn et al. 2003). In peaches, proteomic analysis of ripe fruit from NMF and MF phenotypes showed that the expression of a protein putatively identifiable as a CAD was significantly higher in NMF than in MF fruit (Prinsi et al. 2011).

On the other hand, besides the conversion of monomeric phenylpropanoids to lignin (insoluble

phenolics), in most plants phenylpropanoids generated from phenylalanine can be further modified in many ways, including their elongation and cyclization to form flavonoids and anthocyanidins (Ververidis et al. 2007). Therefore, a metabolic interaction between anthocyanin and lignin biosynthesis (at different steps during the whole process) and possible redirectioning of the polyphenols metabolic pathway/s can be hypothesized (Thévenin et al. 2011, van der Rest et al. 2006). Concerning fruit, in peach a possible competition between flavonoid and lignin biosynthesis has also been hypothesized (Dardick et al. 2010). In strawberry, induction of a FaPRX27 peroxidase (assumed to be involved in lignin formation) concomitant with down-regulation of the chalcone synthase gene during fruit ripening diverts the metabolic flux from anthocyanins to lignin (Ring et al. 2013), highlighting the possibility of a competition of the different phenolics pathways for common precursors.

The complex interplay of enzymes involved in the different branches of the phenylpropanoid pathway is further complicated by their possible role in divergent pathways, alternative to lignin biosynthesis. In *Arabidopsis thaliana* the aldehyde dehydrogenase Reduced Epidermal Fluorescence (REF1; Nair et al. 2004) is capable to oxidize the same substrates (cinnamaldehydes) reduced by CAD to monolignols producing ferulic and syringic acids. Ferulic acid may in turn affect the stiffness of the cell wall as described for Chinese water chestnut (Waldron et al. 1997), where the thermal stability of cell adhesion and maintenance of crispness after cooking have been ascribed to diferulic acid cell-wall crosslinks. Also in other monocots ferulic acid could be involved in cell wall stiffening (Ralph 2010). Another recently described *A. thaliana* mutant, *ref8*, impaired in lignin biosynthesis, accumulates higher levels of salicylic acid than the wild type (Kim et al. 2014).

Many of these enzyme activities appear to be affected by the plant regulator ethylene (Kirch et al. 2004, Mita et al. 2006), deeply involved in the control of ripening in climacteric fruits, category to which peach belongs (Tonutti et al. 1996, 1997).

The present work investigated whether fruit of peach cultivars with different flesh firmness and/or color (yellow/red-purple) presented differences, at the molecular and biochemical levels, in CAD expression and activity, also in relation to the possible involvement of CAD in the determination of the contents of lignin, anthocyanins, and total phenolics. To our knowledge, this issue, different than in other fruits, has never been addressed to in peach.

The peach genotypes studied included the yellow-fleshed NMF ‘Oro A’ and MF ‘Springcrest’, and the blood-flesh MF ‘Sanguinella’, a local cultivar present in Central Italy showing early accumulation of anthocyanins in the mesocarp during fruit development (Shen et al. 2013 and references therein) and promising for its future introduction in selection programs addressed to the obtainment of peach genotypes with enhanced antioxidant contents.

Materials and methods

Plant material and fruit sampling

‘Springcrest’ peach [*Prunus persica* (L.) Batsch] trees were grown in the Experimental Orchard “Francesco Dotti” of the University of Milan (Italy), whereas ‘Oro A’ and ‘Sanguinella’ trees were grown in the Experimental Orchard of the University of Bologna [Italy; Department of Agricultural Sciences (DiSTA)]. Trees were subjected to standard horticultural practices.

Growth of peach fruit (2012 spring-summer season) was monitored at regular intervals starting at 35 days after full bloom (DAFB). Growth stages were defined according to Tonutti et al. (1997). At the desired times, fruit were picked and quickly transferred to the laboratory for the determination of weight and ripening parameters (flesh firmness, epicarp colour, total soluble solids contents and ethylene emission). On the basis of fruit weight, epicarp colour and ethylene emission, homogeneous fruit classes were pooled for sampling. Fruit mesocarp was isolated by removing peel, stone and the layer of mesocarp (2-5 mm thickness) immediately adjacent to peel and stone, snap-frozen in liquid N₂ and stored at -80°C.

Epicarp colour, ethylene emission, flesh firmness, total soluble solids contents

Epicarp colour parameters were measured, on two opposite, non blushed sides in the fruit equatorial zone, by a Konica Minolta Chroma Meter CR-400 reflectance colorimeter (Konica Minolta Co., Osaka, Japan). Only the a* index value, which records the ratio of green (negative values) to red (positive values) pigmentation according to the CIE L*a*b* scale, was taken as representative of ripening degree (McGuire 1992, Robertson et al. 1990). Fruit ethylene emission was evaluated, within two hours from harvest, by placing individually, in 1.1-l glass jars in a thermoregulated (20 ± 1°C) chamber with 95% relative humidity, whole, healthy fruits whose weight and colour matched the average values (± 10%) defined for the desired ripening classes. Ethylene analysis was conducted by gas-chromatography [gas-chromatograph Model 3800; DANI Instruments, Cologno Monzese, Italy, equipped with a stainless steel column (100 cm long; 0.32 cm diameter) filled with Porapack Q at 100° C and a flame-ionisation detector, at 210° C, with nitrogen at 0.8 bar as carrier gas] on 1-ml gas samples collected from the headspace of the jars after 1 h of hermetic closure (Benedetti et al. 2008). Each peach sample was evaluated three times and average of the results was used for the statistical analysis; data were expressed as nl of ethylene h⁻¹ g⁻¹ FW. Flesh firmness was measured by a hand penetrometer (8 mm flat probe, Effegi, Alfonsine, Italy) after peel removal. Two determinations, one for each cheek, were performed on each fruit; data were expressed in Newton (N). The SSC content of the mesocarp cell sap was evaluated with a hand-held refractometer (ATAGO Co. Ltd., Tokyo, Japan) conducting two determinations on each fruit; data were expressed in degrees Brix (°Brix).

Total phenolics

Total phenolics contents were measured with Folin-Ciocalteu's phenol reagent as described in Scalbert et al. (1989). One gram of frozen mesocarp was ground to powder with liquid N₂, added with 4 ml of aceton:methanol:water (2:2:1) plus 1% (v/v) acetic acid and shaken 15 min at room temperature (RT). After centrifugation (15 min, 5000 g), supernatants were collected and the precipitates washed twice with 2 ml of the same extraction solution. The collected supernatants were finally brought to 10 ml with the same extraction solution. Gallic acid standards (3-20 µg) and samples (0.1 ml) were diluted with double-distilled water (7.9 ml), added with 0.5 ml of 50% (v/v) Folin-Ciocalteu's reagent plus 1.5 ml saturated Na₂CO₃, vigorously shaken and incubated for 2 h at RT before absorbance measurement at 765 nm against blank. Total phenolics contents were expressed as gallic acid equivalents on a fresh weight basis (mg g⁻¹ FW).

Total anthocyanins

Anthocyanin pigments were extracted according to Lee et al. (2005) with some modifications. Two grams of frozen mesocarp were ground to powder with liquid N₂, added with three volumes of 95% (v/v) EtOH:1.5 M HCl (85:15), mixed thoroughly and shaken overnight at 4°C. Samples were centrifuged (40 min, 10 000 g, 4°C) and the supernatants collected. Five volumes of 100% hexane were added to a fraction of each sample, that was vigorously shaken and allowed to stand for 30 min on ice. The aqueous lower phase was collected and diluted in two different buffers, at pH 1.0 [0.025 M KCl in 95% (v/v) EtOH] and pH 4.5 [1 M Na-acetate in 95% (v/v) EtOH]. Absorbance (Abs) of the samples was determined at 520 nm and 700 nm in both pH conditions and calculated as follows:

$$A = (\text{Abs}_{520} - \text{Abs}_{700})_{\text{pH } 1.0} - (\text{Abs}_{520} - \text{Abs}_{700})_{\text{pH } 4.5}$$

The amount of total anthocyanins was calculated as described by Lee et al. (2005) (molar extinction coefficient ε = 26900 1 mol⁻¹ cm⁻¹ for cyanidin-3-glucoside; molecular weight for cyanidin-3-glucoside: 449.2 g mol⁻¹) and expressed as cyanidin-3-glucoside equivalents on a fresh weight basis (mg g⁻¹ FW).

Lignin determination

Lignin determination was conducted according to Cai et al. (2006a) with slight modifications. Frozen mesocarp tissue (3 g) was ground with liquid N₂, added with 6.5 volumes of extraction buffer [100 mM K₂HPO₄/KH₂PO₄ pH 7.8, 0.5% (v/v) Triton X-100, 0.5% (w/v) polyvinylpyrrolidone], shaken (200 rpm) for 30 min at RT, and centrifuged (20 min, 6000 g, RT). Precipitates were washed twice in the same conditions, followed by four additional washings with 20 ml of 100% MetOH, and dried overnight at 80°C. Fifty mg of these dried precipitates were used for lignin determination, in parallel with lignin alkali standards (50 mg lignin, average Mw 10 000; Sigma-Aldrich, Milan, Italy). Samples were added with 5 ml of 2 N HCl plus 0.5 ml of 100% thioglycolic acid, heated (4 h, 100°C), cooled on ice and centrifuged (20 min, 20 000 g). The precipitates, rinsed three times with distilled water and resuspended in 5 ml of 1 M NaOH, were shaken for 18 h at 200 rpm and centrifuged (20 min, 20 000

g). One hundred μl of concentrated HCl were added to 0.5 ml of each recovered supernatant, and the lignin-thioglycolic acid complex was precipitated by cooling (4 h, 4°C) and centrifuging (20 min, 20 000 *g*). The precipitates were then dissolved in 1 ml of 1 M NaOH and, after proper dilution, their absorbance at 280 nm (Abs_{280}) was read against a blank. Data were calculated against a lignin alkali standard curve and expressed on a fresh weight basis (mg g^{-1} FW).

Protein extraction

Soluble protein extraction was conducted as described by Cai et al. (2006a), with minor modifications. Fruit mesocarp (1.5 g) was ground with liquid N₂ in the presence of 10% (w/w) polyvinylpolypyrrolidone (PVPP). Two volumes of ice-cold extraction buffer [250 mM Tris(hydroxymethyl)aminomethane (Tris)-HCl, pH 7.5, 2 mM MgCl₂, 10% (v/v) glycerol, 2 mM dithiothreitol (DTT), 10 mM β -mercaptoethanol (β -MSH), 1 μM leupeptin, 1 mM phenyl-methyl-sulfonyl-fluoride (PMSF)] were added, and the thawed slurries were sonicated (three times, 15 s, 20 W; Microson Ultrasonic Cell Disruptor XL, Misonix Inc., Farmingdale, NY) and centrifuged (15 min, 23 000 *g*, 4°C). The resulting supernatants were used immediately for the determination of in vitro CAD activity or stored (-80°C) for subsequent polyacrylamide gel electrophoresis (PAGE) analyses.

In vitro assay of CAD activity

In vitro CAD activity was assayed as described by Mansell et al. (1974) by monitoring spectrophotometrically (Varian Cary 50 Bio UV/ Visible Spectrophotometer, Agilent Technologies Italia SpA, Cernusco s/Naviglio, Italy), the formation of coniferyl aldehyde from coniferyl alcohol through the increase in absorbance at 400 nm at 37°C for 3 min. Aliquots (25-100 μl) of fruit tissue extract were added to a 1-ml final volume of assay medium (100 mM Tris-HCl buffer, pH 8.8, 0.2 mM coniferyl alcohol, 0.2 mM NADP⁺). One unit (EU; enzyme unit) of CAD activity was defined as the amount of enzyme that caused the change in Abs_{400} of 0.01 per minute under the specified conditions. The data are expressed on a protein basis.

Protein determination

Protein content was determined by the Bradford method (Bradford 1976) using bovine serum albumine (BSA, Sigma-Aldrich) as a standard (Micro-Bio-Rad Protein Assay, Bio-Rad Laboratories, Segrate, Italy).

SDS-PAGE

Proteins denatured in SDS sample buffer (Laemmli 1970) were analysed by tricine-SDS-PAGE (10% total acrylamide/bis-acrylamide concentration; Schägger and von Jagow 1987) in a MiniProtean™ apparatus (Bio-Rad Laboratories); gels were stained with Coomassie Blue R-250. Molecular weight markers were from Bio-Rad (Kaleidoscope Pre-Stained Standards).

Nondenaturing PAGE and in gel CAD activity

Nondenaturing PAGE was performed at 4°C in a MiniProtean™ apparatus as described in Laemmli (1970) and in Mansell et al. (1974), with minor modifications. The separating gel contained 9.83% (w/v) acrylamide, 0.27% (w/v) methylene-bisacrylamide in 375 mM Tris-HCl, pH 8.8 plus 6% (v/v) glycerol, and the stacking gel contained 3.9% (w/v) acrylamide, 0.1% (w/v) methylene-bisacrylamide in 125 mM Tris-HCl, pH 6.8. Polymerisation was triggered by addition of ammonium persulfate (APS) and N,N,N',N'-tetramethylethylenediamine (TEMED). The sample buffer was composed of 62.5 mM Tris-HCl, pH 6.8, 10% (w/v) glycerol, 0.01% (w/v) pyronin Y. The tray buffer consisted of 25 mM Tris plus 192 mM glycine. After the run, gels for activity staining (Umesh and Kavitha 2011) were equilibrated twice at 30°C for 15 min in 100 mM Tris-HCl, pH 8.8 and incubated still for additional 4 h at 30°C in 10 ml of activity buffer (100 mM Tris-HCl, pH 8.8, 0.1 mg phenazinemethosulphate, 2.5 mg nitrobluetetrazolium, 2.5 mg coniferyl alcohol or 0.025% ethanol (as negative control). CAD activity was visually assessed by colour evolution.

Western blotting

After SDS-PAGE, proteins were electroblotted onto PVDF membrane in a Multiphor II Nova-Blot (Amersham Biosciences, Milan, Italy) apparatus (Morgutti et al. 2006). After nondenaturing PAGE, gels were conditioned with three washes (10 min each) in 25 mM Tris-HCl, pH 8.8, 192 mM glycine, 20% (v/v) MetOH, 0.1% (w/v) SDS; subsequent electroblotting was performed in the presence of the same buffer without SDS. Protein transfer was carried out at 4°C (nondenaturing gels) or RT (SDS-PAGE) at 0.8 mA cm⁻². Membranes were blocked for 2 h at the same temperature of transfer in 5% (w/v) BSA in Tris buffered saline-Tween buffer [TBS-T: 20 mM Tris-HCl, pH 7.6, 200 mM NaCl, 0.05% (w/v) Tween-20] and incubated overnight at 4°C with the anti-CAD antisera diluted in TBS-T plus 1% (w/v) BSA [1:3000 for anti-FaCAD antibodies; 1:10 000 for anti-*Prunus persica*_CAD sc8 (anti-PRUPE_CAD sc8)]. Blots, thoroughly washed with TBS-T, were incubated (2 h, RT) with anti-rabbit alkaline phosphatase-conjugated secondary antibodies and detection was achieved with SIGMAFAST™ BCIP®/NBT tablets (Sigma-Aldrich).

Anti-CAD antibodies

Polyclonal antibodies raised against the recombinant CAD1 protein of *Fragaria × ananassa* (FaCAD, AAK28509.1, Blanco-Portales et al. 2002) were a kind gift of prof. Rosario Blanco-Portales (University of Cordoba, Spain).

PRUPE_CAD amino acid sequences, deduced from the Peach Genome sequence (Verde et al. 2013), were aligned using the Clustal W 2.1 program under the default settings (Larkin et al. 2007) to identify an amino acid sequence peculiar of one (PRUPE_ppa007736m; residues 114-128: CNKKIWSYNDTYSDG) of the two putative CAD proteins encoded by the PRUPE_CAD genes on

scaffold 8. The selected sequence, evaluated by Epitopia server (Rubinstein et al. 2009) for immunogenicity, was used to synthesize the corresponding $\text{^2HN-CNKKIWSYNDTYSDG-COOH}$ peptide. This was conjugated with keyhole limpet hemocyanin (KLH) to raise polyclonal antibodies in rabbits (Primm s.r.l. Company, Segrate, Italy). Pre-immune and immune antisera (collected 48 d after inoculation and tested for antibody titre) were used for Western blot analyses.

RNA extraction and quantification, and semiquantitative RT-PCR analysis

RNA extraction was conducted as described in Tong et al. (2012) with slight modifications. One gram of frozen mesocarp tissue was ground to powder with liquid N₂ in the presence of 2% (w/w) PVPP, plus 0.8 ml of preheated (65°C) extraction buffer [2.5% (w/v) cetyltrimethylammonium bromide (CTAB); 100 mM Tris-HCl, pH 8.0; 25 mM Na₂-EDTA; 2 M NaCl; 5% (v/v) β-MSH], thoroughly vortexed for 30 s and incubated for 30 min at 65°C with vortexing every 5 min. Samples were centrifuged (3 min, 5000 g, 4°C) and the supernatants were added with one volume of chloroform:isoamyl alcohol (24:1, v:v), vigorously mixed for 30 s and centrifuged (12 min, 13 000 g, 4°C). The recovered top phase, was added with one volume of phenol:chloroform:isoamyl alcohol (25:24:1, v:v:v), incubated on ice for 10 min and centrifuged. The procedure was repeated twice. The recovered top phase was added with one volume of ice-cold 5 M NaCl, mixed, added again with one volume of ice-cold 100% (v/v) isopropyl alcohol, mixed, and kept at -20°C for at least 30 min. After centrifugation (12 min, 13 000 g, 4°C), the precipitates were dried under vacuum and resuspended in 0.6 ml of Tris-EDTA buffer (10 mM Tris-HCl, pH 8.0, 1 mM EDTA) in the presence of 3 M LiCl. After overnight incubation at 4°C; samples were centrifuged (20 min, 13 000 g, 4°C) and the precipitates, washed with ice-cold 70% (v/v) EtOH, were dried under vacuum and resuspended in 30 µl of diethylpyrocarbonate (DEPC)-treated water.

RNA samples were loaded onto agarose gels [1% (w/v) agarose plus 1 µg ml⁻¹ ethidium bromide] to verify their integrity, and quantitated (NanoDrop 2000c spectrometer, Thermo Fisher Scientifics Inc., Waltham, MA). 3.5 µg of RNA from each sample were treated with RNase-free DNase I (Invitrogen Life Technologies, Monza, Italy); 2.6 µg of DNase I-treated RNA was subjected to retrotranscription with the commercial RT-PCR kit SuperScript® III Reverse Transcriptase (Invitrogen). The cDNAs obtained were immediately divided into aliquots and stored at -20°C. Semi-quantitative RT-PCR analyses were performed using gene-specific or degenerated primers and Taq polymerase (GoTaq®, Promega, Segrate, Italy). The cycling parameters were: 5 min preliminary denaturation at 94°C; 27 (PRUPE_S16/PRUPE_ppa012996mg) and PRUPE_ACO1/PRUPE_ppa008791mg) or 35 (all considered PRUPE_CAD genes) denaturation cycles (45 s at 94°C), annealing (1 min at primer-specific melting temperature; see Appendix S1 in Supporting Information), extension (2 min at 72°C) and a final extension of 5 min at 72°C. PCR products were separated in 1% (w/v) agarose gels.

Primer design

Gene-specific or degenerated primers were designed with the help of Primer3 web resource (Rozen and Skaletsky 2000; <http://bioinfo.ut.ee/primer3/>). For *PRUPE_CADs sc6*, primers able to amplify the highest possible number of *PRUPE_CAD sc6* isogenes (i.e. *PRUPE_ppa007622mg*, *PRUPE_ppa007613mg*, *PRUPE_ppa007226mg*, *PRUPE_ppa016455mg*, *PRUPE_ppa007668mg*) were used. For *PRUPE_CAD sc8*, degenerated primers able to amplify both *PRUPE_CAD sc8₁* (*PRUPE_ppa007749mg*) and *PRUPE_CAD sc8₂* (*PRUPE_ppa007636mg*) isogenes were used (see Appendix S1 in Supporting Information).

Bioinformatic and phylogenetic analysis

Sequences used for the in silico analysis of *CAD* genes were retrieved from the National Center for Biotechnological Information (NCBI; <http://www.ncbi.nlm.nih.gov/>), Phytozome (<http://www.phytozome.org>) and the SIB Bioinformatics Resource Portal ExPASy (<http://www.expasy.ch>) databases. Comparison analysis of all the sequences identified in the Peach Genome was conducted with the advanced Basic Local Alignment Tool BLAST X (Altschul et al. 1990) at NCBI as well as in the Universal Protein Resource database (UniProt; <http://www.uniprot.org>). The amino acid sequence alignments were used to generate a phylogenetic tree based on the Neighbor-joining algorithm (Saitou and Nei 1987) and the resulted ‘phenogram’ was created using the MEGA 4.0 program (Tamura et al. 2007; <http://www.megasoftware.net/mega4/mega.html>). Reliability was inferred using the bootstrap method with 1000 replicates.

Molecular weights and isoelectric points were predicted using the ExPASy data base tools.

Statistical analysis

ANOVA and Bonferroni’s tests were calculated with Sigma-Stat for Windows (Version 3.11) using the values of means and standard errors (SE) for each parameter.

Results

Fruit phenotypization: epicarp colour, growth, ethylene emission, flesh firmness, total soluble solids

Prunus persica fruit of NMF ‘Oro A’, MF ‘Springcrest’ and MF ‘Sanguinella’ cultivars were picked at the desired ripening stages, i.e., S3, S4 I (pre-climacteric), S4 III (climacteric), as individuated by monitoring fruit development from full bloom. Figure 1 shows the fruit visual appearance in S4 III (Fig. 1A-C) and the values of colour index a^* (Fig. 1D) and of average fruit weight (Fig. 1E). In the S4 III final stage of ripening, NMF ‘Oro A’ fruit showed a definite yellow colour of the epicarp, in MF ‘Springcrest’ the skin was for the largest part dark red, and MF ‘Sanguinella’ showed only a slight red shade over greenish background in the markedly hairy skin (Fig. 1A-C). During fruit ripening the colour index a^* increased in all cultivars, but its absolute values were very different. In MF ‘Sanguinella’ fruit the values of a^* index were positive already at Stage S3, but the final value was at Stage S4 III essentially equal to that of NMF ‘Oro A’ (Fig. 1D). ‘Oro A’ fruit were the smallest and their weight did not increase greatly from Stage S3 to S4 III; a similar behaviour, although starting from a higher average weight at S3, was apparent in ‘Sanguinella’ fruit in the transition from S3 to S4 III. ‘Springcrest’ fruit showed the largest growth increase reaching at Stage S4 III the largest size (Fig. 1E).

Fruit whose weight and epicarp colour were closer to the mean values of the three ripening stages were chosen to evaluate ethylene emission. ‘Oro A’ fruit produced ethylene in little amounts already in Stage S3, with a slight increase between Stages S3 and S4 I and a dramatic increase between S4 I and S4 III. In ‘Springcrest’, ethylene emission became detectable only in S4 I, with a sharp increase, although to levels lower than in ‘Oro A’, between Stages S4 I and S4 III. A similar behaviour was observed in ‘Sanguinella’, where ethylene emission was much lower than in the two other cultivars (Figure 2).

Fruit were also phenotypized for flesh firmness and total soluble solids (SSC; Fig. 3). Fruit firmness was low in ‘Oro A’ fruit already at the S3 Stage, and it decreased gradually reaching at S4 III the value of approx. 23 N. In ‘Springcrest’, flesh firmness was higher in S3, but it decreased sharply between S3 and S4 I and furthermore so in the transition between S4 I and S4 III. A similar trend was apparent for ‘Sanguinella’, where flesh firmness values in S4 III were even lower than in ‘Springcrest’ at the same stage (Fig. 3A).

The levels of total SSC, as expected, increased with ripening in all three cultivars, being lowest in all three stages of ripening in ‘Springcrest’, higher in ‘Oro A’ and highest in ‘Sanguinella’ (Fig. 3B).

Total phenolics, anthocyanin and lignin contents in the flesh

Figure 4 shows the changes in the levels of three different classes of phenolic compounds (i.e., total phenolics, anthocyanins and lignin) with the advancement of ripening in fruit of the three peach

cultivars studied. The amounts of total phenolics and the changes in their levels were different in NMF ‘Oro A’ compared to MF ‘Springcrest’ and MF ‘Sanguinella’ (Fig. 4A). In ‘Oro A’ fruit, the levels of total phenolics were lowest and constant in the three phases of ripening, whereas in ‘Springcrest’ their levels, highest in S3, decreased with the advancement of ripening. ‘Sanguinella’ showed levels of total phenolics almost two-fold higher than those of ‘Springcrest’ at all stages, that decreased with ripening. Anthocyanins, that were undetectable in the flesh of both ‘Oro A’ and ‘Springcrest’, were present in ‘Sanguinella’ and their levels decreased with ripening (Fig. 4B).

Flesh lignin contents, expressed on a fresh weight basis (Fig. 4C), were lower in NMF ‘Oro A’ and higher in MF ‘Springcrest’ and MF ‘Sanguinella’. In all cultivars a decrease with ripening was observed (Fig. 4C).

In vitro CAD activity

To our knowledge, no data are at the present time available in the literature concerning CAD activity in peach fruit; therefore, we assayed the in vitro CAD activity in the mesocarp of fruit of NMF ‘Oro A’, MF ‘Springcrest’ and MF ‘Sanguinella’ at the three stages of ripening. In ‘Oro A’ fruit no CAD activity was detectable in Stages S3 and S4 I, that became apparent only at Stage S4 III. In the flesh of ‘Springcrest’ fruit, no CAD activity could be detected in any ripening stage; very high CAD activity, that increased with ripening, was measured in the flesh of ‘Sanguinella’ already in Stage S3 (Figure 5).

Identification and phylogenetic relationship analysis of *PRUPE_CAD* genes in the *P. persica* genome, and alignment of the deduced *PRUPE_CAD* protein sequences

Annotated *CAD* sequences of different plant species were retrieved in NCBI and ExPASy databases and aligned on Peach Genome (Phytozome database) using BLAST. A large *PRUPE_CAD* gene family was identified, whose components are present in six (1, 3, 4, 5, 6, 8) of its eight scaffolds. From these gene sequences a dataset of deduced peach *PRUPE_CAD* proteins was obtained. Only 24 sequences composed of more than 280 amino acid residues were selected as putative functional CADs, on the basis of the medium size (approx. 300 amino acid residues) of proteins of the CAD family (Strommer 2011). In silico analyses allowed to individuate 32 additional “short” sequences probably referring to non-functional polypeptides (data not shown).

The deduced putative *PRUPE_CAD* sequences were aligned and their reciprocal identity scores determined (CLUSTAL W 2.1 multiple sequence alignment software; see Appendix S2 in Supporting Information). Sequence alignment revealed that the functional CAD motifs (Deng et al. 2013 and references therein) were present in the great majority of isoforms: the NADPH binding motif [GXG(X)₂G] was present in all isoforms; the Zn2 [GD(X)_{9..10}C(X)₂C(X)₂C(X)₇C] binding motif was absent only in *PRUPE_CADs* sc6_{10,15}; the Zn1 [GHE(X)₂G(X)₅G(X)₂V] binding motif was altered only in *PRUPE_CADs* sc6_{11,13}. The reciprocal identity among the *PRUPE_CADs* of scaffolds 1, 3-5 was on average approx. 50%, and that of these isoforms with of the *PRUPE_CADs* sc6, taken as a

whole, was of 53% (PRUPE_CAD sc1), 49% (PRUPE_CAD sc3), 64% (PRUPE_CAD sc4), and 50% (PRUPE_CAD sc5). The PRUPE_CADs of scaffolds 1, 3-5 showed an average identity score <50% with the PRUPE_CADs sc8. Concerning the 18 PRUPE_CADs sc6, there was a reciprocal identity score ≥85% among the six isoforms PRUPE_CADs sc6_{1-5,18}; compared to PRUPE_CAD sc6₁ (taken as a reference), the seven isoforms PRUPE_CAD sc6_{6-11,13} showed identity scores between 75% and 83%, whereas the five isoforms PRUPE_CAD sc6_{10,12,14,16,17} showed identity scores between 48% and 71%. The two putative PRUPE_CADs sc8_{1,2} had a reciprocal identity score of 85.7%, and resulted quite different than the reference PRUPE_CAD sc6₁, with an average identity score of 51%. The putative PRUPE_CAD sc8₂ encoded by the *PRUPE_ppa007636mg* gene of scaffold 8 seemed particularly interesting on the basis of its 100% identity with the putative CAD polypeptides identified in peach fruit (Prinsi et al. 2011).

In order to investigate the phylogenetic relationships of PRUPE_CADs with those of other plant species with described biochemical/physiological functions, the 24 putative PRUPE_CAD sequences were subjected to phylogenetic analysis (MEGA 4.0 software and Neighbor-joining data clustering). The phylogenetic tree (Fig. 6) showed three, highly supported clusters (bootstrap test, 1000 replicates) corresponding to the three classes (I-III) recently proposed (Deng et al. 2013 and references therein). The PRUPE_CADs grouped within Classes I (PRUPE_CADs sc8_{1,2} and PRUPE_CAD sc6₁₂) and III (all the other PRUPE_CADs sc6 plus PRUPE_CAD sc1 and PRUPE_CADs sc3-5). In particular, PRUPE_CAD sc6₅ showed maximum phylogenetic proximity with the strawberry FaCAD (AAK28509.1; Blanco-Portales et al. 2002), confirmed also by the highest identity score (88.6%) between the two sequences (see Appendix S3 in Supporting Information).

On the basis of the results of Fig. 6, we restricted the analysis to PRUPE_CAD sc6₅ and PRUPE_CAD sc8₂. The deduced amino acid sequences of these two putative PRUPE_CAD isoforms were aligned with those of CADs: a) present in fruits with peculiar characteristics of flesh firmness, i.e. FaCAD, EjCAD1 (ABV44810.1 from *E. japonica*; Shan et al. 2008) and PmCAD (BAE48658.1 from *Prunus mume*; Mita et al. 2006); b) with acknowledged involvement in lignin biosynthesis, i.e., AtCAD4 and AtCAD5 (AAP59434.1 and AAP59435.1 from *A. thaliana*; Sibout et al. 2003); c) possibly involved in defense-related responses, i.e. CsCAD2 (ADO51749.1 from *Camellia sinensis*; Deng et al. 2013) (Fig. 7). Identity scores showed that, apart from the already described high identity with the considered FaCAD, PRUPE_CAD sc6₅ had very low identity with the CADs from other species (approx. 50% identity with the AtCAD4 and AtCAD5 proteins and 6%-9% with CsCAD2, EjCAD1 and PmCAD). PRUPE_CAD sc8₂ showed high (approx. 78%) identity with AtCAD4 and AtCAD5, and much lower (approx. 6%) identity with EjCAD1, PmCAD and CsCAD2.

Levels of PRUPE_CAD sc6 and PRUPE_CAD sc8 isoforms and in gel CAD activity

The high identity scores (64%-89%) between the FaCAD and the putative PRUPE_CADs sc6 (see Appendix S3 in Supporting Information) allowed to consider polyclonal anti-FaCAD antibodies

(Blanco-Portales et al. 2002) useful to recognize all the PRUPE_CADs sc6. This hypothesis was verified in preliminary experiments that probed with the anti-FaCAD antibodies the soluble proteins of the lignifying endocarp of Stage S2 ‘Springcrest’ peaches. In this material, where a high in vitro CAD activity could be detected, a strong immunoreaction signal against a polypeptide of approx. 40 kDa could be observed (data not shown), consistent with the value reported for monomers of the active CAD dimer (O’Malley et al. 1992) and with the average one (38.4 kDa) deduced for the PRUPE_CAD sc6 translation products (Appendix S4 in Supporting Information). Polyclonal antibodies were also raised against the specific isoform PRUPE_CAD sc8₂ exploiting a peculiar (respect to 17 out of the 18 PRUPE_CADs sc6) and satisfactorily immunogenic (Epitopia tool; Rubinstein et al. 2009) 15-amino acid sequence (₁₁₄CNKKIWSYNDTYS₁₂₈DG; Fig. 7 and Materials and methods section).

Western blot experiments were conducted probing with the two different anti-CAD antibodies the soluble proteins from the flesh of fruit of each cultivar at the three stages of ripening after separation by SDS-PAGE (Fig. 8). The putative PRUPE_CAD sc6 polypeptides were essentially undetectable in all of the three cultivars at all ripening stages, whereas polypeptides of approx. 40 kDa (again consistent with the values deduced also for the PRUPE_CADs sc8; Appendix S4 in Supporting Information) were recognized by the anti-PRUPE_CAD sc8 antibodies. The PRUPE_CAD sc8 polypeptides were detectable in ‘Oro A’ only at Stage S4 III, essentially absent in ‘Springcrest’ at all stages of ripening, and present in ‘Sanguinella’ already in Stage S3 in relatively high amounts apparently increasing with ripening.

Twenty out of the 24 PRUPE_CADs had deduced pIs minor than 7.0 (Appendix S4 in Supporting Information), consistent with what generally reported for these proteins (Mansell et al. 1974). Therefore, it was possible to conduct experiments in native gel conditions suitable for acidic proteins analysis. The availability of antibodies able to discriminate between different putative PRUPE_CAD isoforms (Fig. 8) made in principle possible to evaluate, in parallel experiments co-localizing the position of CAD activity bands with the immunoreaction signals, whether the different PRUPE_CADs contributed differently to the in vitro “bulk” CAD activity (Fig. 5). Colour development due to CAD activity in ‘Oro A’ fruit was essentially absent in Stages S3 and S4 I, but it became clearly detectable at Stage S4 III. Essentially no CAD activity could be seen in ‘Springcrest’ at all three stages considered, whereas in ‘Sanguinella’ CAD activity was already detectable at Stage S3 and increased in Stages S4 I and S4 III. These data appear consistent with those regarding the in vitro “bulk” CAD activity from the different fruit (Fig. 5). Western blot results indicate that, where present, in gel CAD activity was due to the contribution of the only PRUPE_CAD sc8 isoforms (Fig. 9).

Expression analysis of the *PRUPE_CAD* genes

The transcript levels of the *PRUPE_CAD sc6*, *PRUPE_CAD sc8* and *PRUPE_ACO1* genes were analyzed (semiquantitative RT-PCR with proper primers; Appendix S1 in Supporting Information)

using the mRNA levels of a ribosomal (*PRUPE_S16*) gene as a reference (Fig. 10). In Stage S3, the *PRUPE_ACO1* transcripts were clearly visible in ‘Oro A’ but almost undetectable in ‘Springcrest’ and ‘Sanguinella’. The levels of *PRUPE_ACO1* transcripts increased with ripening in all three genotypes, according to fruit ethylene emission (Fig. 2).

Concerning the large group of *PRUPE_CAD sc6* genes, primers able to amplify the highest possible number of components of this group (i.e. *PRUPE_CADs sc6₁₋₅*; Appendix S1 in Supporting Information) were chosen. Transcripts of *PRUPE_CADs sc6₁₋₅* did not at all (‘Oro A’ and ‘Springcrest’), or only slightly (‘Sanguinella’) accumulate in the fruit mesocarp at the ripening stages considered. Expression of the two *PRUPE_CAD sc8_{1,2}* genes was clearly detectable in fruit from all cultivars, and particularly high in ‘Oro A’. The levels of *PRUPE_CAD sc8_{1,2}* transcripts were essentially constant through Stages S3-S4 III in ‘Oro A’ and increased with ripening in both ‘Springcrest’ and ‘Sanguinella’.

Discussion

Characterization of *P. persica* fruit of ‘Oro A’, ‘Springcrest’, and ‘Sanguinella’ at harvest, on the basis of ethylene emission (Fig. 2) and flesh firmness (Fig. 3), allowed to categorize them into the desired ripening stages confirming phenotypic (NMF/MF) typologies. The literature describes for peach fruit four ripening stages (S1-S4), thoroughly defined for ‘Springcrest’ peaches by Tonutti et al. (1997). In this cultivar the highest rates of ethylene emission are detectable during early fruit growth (Tonutti et al. 1991) and at Stage 4 of ripening (Tonutti et al. 1996). In general, during ripening of climacteric fruits such as tomato, passion fruit and kiwifruit, *ACO* transcripts appear prior to the burst of ethylene emission (Mita et al. 1998, Nakatsuka et al. 1997, Zhong et al. 1998); also in peach, *ACO* transcripts are massively accumulated when ethylene emission is still very low (Tonutti et al. 1997). Fruit of the genotypes studied in the present work showed a consistent behaviour: *PRUPE_ACO1* transcripts were apparent in all three genotypes at Stage S4 I, when ethylene emission was still extremely low; in ‘Oro A’ *PRUPE_ACO1* transcripts could be clearly detected already at Stage 3 (compare Figs. 10 and 2). Fruit ethylene emission appeared earlier and was greater in ‘Oro A’ than in ‘Springcrest’ and in ‘Sanguinella’ (Fig. 2), consistent with reports showing that NMF peaches generally evolve higher amounts of ethylene than MF ones (Brovelli et al. 1999, Kao et al. 2012, Morgutti et al. 2005, 2006).

NMF peaches are distinguished from MF ones since, although softening, they do not undergo the rapid loss of firmness typical of the “melting” phase (Lester et al. 1996). In the three genotypes studied, although an apparent paradox could be seen among the values of flesh firmness recorded at Stage 3, significantly lower in NMF ‘Oro A’ than in MF ‘Springcrest’ and MF ‘Sanguinella’, the flesh firmness of NMF ‘Oro A’ fruit did not change significantly between Stages S3 and S4 I, and decreased less steeply than in MF ‘Springcrest’ and MF ‘Sanguinella’ between S4 I and S4 III (Fig. 3A), consistent with the reported narrower changes in firmness of NMF fruit compared to MF ones (Bassi and Monet 2008, Shinya et al. 2013). Moreover, for MF peaches a higher softening rate in post-harvest has been described in early-season compared to late-season cultivars (Lurie et al. 2013). Consistent behaviour was observed during ripening also in the presently studied MF fruit, with a slightly steeper softening in the transition from S3 to S4 I in the early-season ‘Springcrest’ than in the late-season ‘Sanguinella’ (Fig. 3A).

The SSC contents, lowest in ‘Springcrest’ and higher in ‘Oro A’ and ‘Sanguinella’ (Fig. 3B), increased during ripening, as expected, in all three cultivars. SSC is an important quality trait in peaches and nectarines being a determinant of consumer’s acceptance and satisfaction. Huge variability in SSC values among peach and nectarine cultivars is reported in the literature; in general, early maturity season varieties show less SSC (Iglesias and Carbó 2009, Legua et al. 2011). Our results show that the early-season cultivar ‘Springcrest’ had the lowest SSC values. The SSC values of ‘Oro A’ are consistent with the features described for fruit of this genotype (Sherman et al. 1990, Prinsi et al. 2011).

The concentrations of total phenolics, anthocyanins and lignin were different in fruit of the three cultivars and changed with ripening (Fig. 4A-C). Besides their adaptive significance (Bravo 1998), the first two classes of molecules macroscopically affect the fruit sensorial qualities in terms of colour (anthocyanins) and astringency (polyphenols), and confer relevant health properties thanks to their antioxidant characteristics, while lignin may contribute to flesh texture. Anthocyanins were detected only in ‘Sanguinella’ according to the features of this blood-flesh genotype (Shen et al. 2013 and references therein). Anthocyanin concentrations usually increase with ripening in flesh and skin of fruits of many species (Jaakola 2013 and references therein), whereas in ‘Sanguinella’ fruit mesocarp they declined constantly from S3 to S4 III. A similar behaviour has been described in pear (Li et al. 2012) and apricot skin, where anthocyanin concentrations decrease in late ripening phases, because of possible degradation or a fruit growth-related dilution effect (Bureau et al. 2009). The concentrations of total phenolics were very different in fruit of the three genotypes considered and remained constant in ‘Oro A’ fruit whereas they decreased with ripening in ‘Sanguinella’ and ‘Springcrest’. These results are, in general, consistent with the reported genotypic variability among peach cultivars and decrease in phenolic contents during peach fruit ripening (Andreotti et al. 2008) and postharvest (Brandelli and Lopes 2005). Similar behaviour has been described in red raspberry (Wang et al. 2009), guava, and other fruits (Bashir et al. 2003 and references therein).

Since in the last phases of ripening of the studied peach fruit the concentrations of total soluble proteins (i.e., on a fresh weight basis) in the fruit mesocarp remained essentially constant (data not shown), it seems possible to exclude that the observed decline in the concentrations of anthocyanins and total phenolics in ‘Springcrest’ and ‘Sanguinella’ be ascribable to a cell enlargement-related dilution effect, or to generalized tissue senescence. In peach, the decrease in polyphenol contents has been related to an increase in polyphenol oxidase activity (Brandelli and Lopes 2005); whether this is the case also in our material needs to be ascertained.

The lignin levels, expressed on a fresh weight basis, decreased with ripening. This apparently paradoxical (taking into account lignin stability) result was corrected if expressed on a per fruit basis (combine Figs. 1D and 4C): in this case, in fact, the lignin levels resulted essentially constant (‘Oro A’ and ‘Sanguinella’), or even increasing (‘Springcrest’) in the transition from Stage S3 to Stage S4 III.

In some fruits, such as loquat, increased flesh firmness is related to increased levels of lignin, in turn related to higher activity of CAD, the last committed enzyme in the synthesis of monolignols, the immediate lignin precursors (Cai et al. 2006a, 2006b, Mansell et al. 1974) and expression of an *EjCAD1* gene (Shan et al. 2008). Similarly, in mangosteen increases in firmness and lignification occur in the pericarp of mechanically damaged fruit (Dangcham et al. 2008). The possibility that also in peach higher flesh firmness may be related to, albeit low, lignification events for increased CAD activity was suggested by the report that putative CAD polypeptides were more abundant in ripe, firm NMF ‘Oro A’ peaches than in softer MF ‘Bolero’ ones (Prinsi et al. 2011).

In Angiosperms, a family of *CAD*-like genes is found, with nine members in *A. thaliana* (Ali

and McNear 2014), 12 in rice (Tobias and Chow 2005), 14 in sorghum (Saballos et al. 2009) and 15 in *Populus* (Barakat et al. 2009). In silico analysis allowed to identify in the Peach Genome 24 putative *PRUPE_CAD* gene sequences. Eighteen of them are found on scaffold 6, two on scaffold 8; one *PRUPE_CAD* gene is located on each of scaffolds 1, 3, 4 and 5. Such a high number of gene copies seems consistent with the hypothesis of the involvement of CAD, also in peach, in functionally redundant metabolic networks in different cell types, tissues, and organs (Kim et al. 2004), with specific functional roles responsive also to developmental and stress conditions (Barakat et al. 2009).

Phylogenetic grouping of CADs from several plant species led to tentative classification considering also their possible different biochemical/physiological roles. The grouping of Fig. 6 follows the criteria suggested by Deng et al. (2013), with CADs belonging to Class I playing a major role in lignin formation (Sibout et al. 2003) and CADs belonging to Classes II and III involved in responses to biotic and abiotic stresses (Barakat et al. 2009).

Our results show that, in the climacteric peach fruit, CAD activity, both in vitro and in gel, increased with ripening, concomitant with increasing ethylene emission (Figs. 2, 5 and 9). This increase seems in general related to increased levels of specific CAD isoforms (*PRUPE_CAD sc8*) and of their gene transcripts (Figs. 8-10). It is well known that the ripening process may be considered in itself a condition of stress accompanied by oxidative, senescence-related events (Seymour et al. 1993). In this view, ethylene may have a function also as a regulator of a ripening-inherent fruit response to stress condition. In peach, possible occurrence of a stress situation in this developmental phase is indirectly suggested by the general decreases, with ripening, in defense mechanisms against oxidative stress (Prinsi et al. 2011) and, as described in the present work, in the concentrations of antioxidant molecules, i.e., total phenolics and anthocyanins, in MF fruit (Fig. 4A). Concerning CAD, experimentally imposed oxidative stress increases the expression of *CAD* genes in strawberry (Aharoni et al. 2002). In the non-climacteric loquat fruit, the expression of *EjCAD1* (whose relative protein grouped in Class II) and the activity of CAD are enhanced upon exposure to low temperature with concomitant occurrence of oxidative stress; these responses are sensitive to ethylene and reversed by ethylene inhibitors (Cai et al. 2006a, 2006b), suggesting an involvement of specific CAD isoforms in the ethylene-mediated response to stress factors. In mangosteen, a CAD protein (ACN38061.1) is produced after mechanical injury, suggesting that this may also be a response to external stress (Bunsiri et al. 2012). The parallelism observed in our material between fruit ethylene emission, CAD activity, *PRUPE_CAD sc8* gene expression and *PRUPE_CAD sc8* protein accumulation may thus be interpreted hypothesizing that these isogenes/enzyme isoforms may play, in ripening peach fruit, a role related to still unraveled mechanism/s of stress response.

PRUPE_CADs sc8 fall in Class I (Fig. 6), proposed to group lignification-related CADs. Nevertheless, in our material the ripening-related increases in *PRUPE_CADs sc8* levels/activity appeared not related to flesh lignification (Figs. 8,9 and 4C). The classification proposed by Deng and coworkers (2013) needs therefore to be considered with some caution, also when considering

PRUPE_CAD sc6. In fact, Figure 6 shows that both the peach putative PRUPE_CADs sc6₁₋₅ and FaCAD, phylogenetically very close (Appendix S3 in Supporting Information), fall in the Class III (stress-response group), whereas their role appears more closely related to lignification processes. The expression of strawberry CAD increases in differentiating vascular elements during achene development in ripening fruit (Aharoni et al. 2002, Blanco-Portales et al. 2002). Concerning PRUPE_CADs sc6, they were present only in the actively lignifying endocarp of Stage 2 'Springcrest' peaches (data not shown), suggesting the hypothesis that these specific isoforms play a role in tissue-specific lignification processes, essentially absent in the mesocarp of either NMF or MF peach fruit.

The lack of protein accumulation in the presence of detectable levels of the corresponding transcripts, as observed for PRUPE_CADs sc8 ('Oro A', S3 and S4 I; 'Springcrest', S3-S4 III) and, to a lesser extent, for PRUPE_CADs sc6 ('Sanguinella' S3-S4 III; Figs. 8-10) may be interpreted by hypothesizing possible post-transcriptional regulatory events related to developmental stage and/or genotype.

The relationship between in vitro CAD activity (Fig. 5) and lignin contents (Fig. 4C) resulted different in peach and loquat fruits (Cai et al. 2006a, 2006b, Shan et al. 2008). Our results show that, in peach, in vitro CAD activity, when present, was much higher than in loquat while the lignin amounts were similar in the two fruits. In our material, lignin levels and CAD activity did not seem unequivocally related. In fact, in 'Oro A' and 'Sanguinella', the lignin contents declined in the transition from Stages S3-S4 III (Fig. 4C), whereas in vitro and in gel CAD activity increased (Figs. 5 and 9). Also in mangosteen the increase in lignin content is not accompanied by increased CAD activity (Dangcham et al. 2008), suggesting again that CAD may not always be directly involved in the production of the polymer. This seems reasonable if one takes into account that the final contents of lignin can also be affected by other reactions, downstream monolignol synthesis, that lead to polymer deposition (Vanholme et al. 2010, 2012). In 'Springcrest', presence of lignin in the mesocarp in the absence of detectable CAD activity (compare Figs. 4C and 5) could be possibly explained as the result of observed presence of high enzyme activity in the early fruit developmental phases S1 and S2 (data not shown).

In peach fruit, differently than what reported in loquat (Cai et al. 2006 a, 2006b), mangosteen (Dangcham et al. 2008), and strawberry (Ring et al. 2013), flesh firmness and lignin contents were not directly related. In fact, firmer NMF 'Oro A' fruit showed in S4 III much lower lignin levels than the softer MF 'Springcrest' and MF 'Sanguinella' ones (Fig. 3A).

The physiological meaning of the very high presence/activity of PRUPE_CAD sc8 and of its corresponding transcripts, that substantially increased with ripening, in the mesocarp of blood-flesh 'Sanguinella' (Figs. 5, 8-10), is presently of difficult explanation. Contrasting reports exist about the possible relationships between anthocyanin and lignin contents and CAD. In *A. thaliana*, hypolignification of stems, related to down-regulation of CAD, parallels accumulation of flavonol glycosides (Thévenin et al. 2011). In strawberry, reduced flux through the anthocyanin/flavonoid

pathway significantly increases lignin content whereas *CAD* expression remains unaffected (Ring et al. 2013). In the white-fleshed strawberry *Fragaria chiloensis*, a tendency to parallel increase in anthocyanin and lignin contents and *CAD* expression has been described (Concha et al. 2013). In blood-flesh ‘Sanguinella’ peaches, anthocyanin and lignin levels in the mesocarp showed the same tendency to decrease during ripening, whereas CAD presence/activity increased. This finding seems to confirm that CADs might play some role diverse than lignification during late fruit ripening. In Japanese apricot a gene encoding a putative CAD is upregulated during ripening in parallel with lack of lignin increase (Mita et al. 2006); its expression in a non-lignifying tissue may be considered as indirect evidence for monolignol-derived, non-lignin end products (Goffner et al. 1998, Lewis and Yamamoto 1990, O’Malley et al. 1992). In vitro cultures of *Linum* species, increased CAD activity was concomitant with lignan accumulation (Fuss 2007). CAD has also been speculated to be involved in the synthesis of cinnamyl alcohol derivatives responsible for fruit flavour (Aharoni et al. 2002 and references herein). Further work is needed to test this hypothesis in blood-flesh peach fruit.

In conclusion, our results allow to exclude that, at least for the cultivars studied, a direct linkage exists in peach fruit between flesh firmness, lignin amounts and CAD activity, and that these are somehow involved in the determination of NMF phenotype.

Unraveling of the precise physiological function of CAD activity, and of the roles of different CAD isoforms, in the mesocarp of ripening peach fruit needs further investigation.

Author contributions

Gabotti Damiano: phenotypization of the experimental material; acquisition, analysis and interpretation of all data. In silico analyses.

Negrini Noemi: phenotypization of the experimental material; substantial contribution to acquisition, analysis and interpretation of in vitro and in gel CAD activity and SDS- and native- PAGE data; contribution to acquisition and interpretation of molecular data, writing of the manuscript.

Morgutti Silvia: phenotypization of the experimental material; substantial contribution to acquisition, analysis and interpretation of in vitro and in gel CAD activity and SDS- and native- PAGE data; contribution to acquisition and interpretation of molecular data; writing of the manuscript.

Nocito Fabio F.: contribution to the design of molecular experiments, interpretation of molecular data, statistical analysis, critical reading of the manuscript.

Cocucci Maurizio: substantial contribution to conception and design of the research, interpretation of data and final approval of the manuscript.

Acknowledgements

This work was supported by a grant from the Italian Ministry of University and Research (MIUR) PRIN-COFIN 2009 prot. 2009SRZRE9: “The determination of nutraceutical and organoleptic features of peach fruit: role of the metabolism of phenylpropanoids and phenolic compounds - Involvement of phenolic compounds in the quality of peach fruit with different phenotype: biochemical and molecular aspects”.

Thanks are due to prof. R. Blanco Portales, University of Cordoba, Spain, for the kind gift of anti-FaCAD antibodies, and to dr. A. Spinardi, DISAA, University of Milan, for ethylene emission measurements in ‘Springcrest’ fruit.

References

- Aharoni A, Keizer LCP, Van Den Broeck HC, Blanco-Portales R, Muñoz-Blanco J, Bois G, Smit P, De Vos RCH, O'Connell AP (2002) Novel insight into vascular, stress, and auxin-dependent and - independent gene expression programs in strawberry, a non-climacteric fruit. *Plant Physiol* 129: 1019-1031
- Ali MB, McNear Jr DH (2014) Induced transcriptional profiling of phenylpropanoid pathway genes increased flavonoid and lignin content in *Arabidopsis* leaves in response to microbial products. *BMC Plant Biol* 14: 84-97
- Altschul SF, Gish W, Miller W, Myers EW, Lipman DJ (1990) Basic local alignment search tool. *J Mol Biol* 215: 403-410
- Andreotti C, Ravaglia D, Ragaini A, Costa G (2008) Phenolic compounds in peach (*Prunus persica*) cultivars at harvest and during fruit maturation. *Ann Appl Biol* 153: 11-23
- Barakat A, Bagniewska-Zadworna A, Choi A, Plakkat U, DiLoreto DS, Yellanki P, Carlson JE (2009) The cinnamyl alcohol dehydrogenase gene family in *Populus*: phylogeny, organization, and expression. *BMC Plant Biol* 9: 26
- Bashir HA, Abu-Goukh BA (2003) Compositional changes during guava fruit ripening. *Food Chem* 80: 557-563
- Bassi D, Monet R (2008) 1 Botany and Taxonomy. In: Layne DR, Bassi D (eds) *The Peach - Botany, Production and Uses*, CAB International, Wallingford, pp 1-36
- Benedetti S, Buratti S, Spinardi A, Mannino S, Mignani I (2008) Electronic nose as a non-destructive tool to characterize peach cultivars and to monitor their ripening stage during shelf-life. *Postharvest Biol Tec* 47:181-188.
- Blanco-Portales R, Medina-Escobar N, Muñoz-Blanco J (2002) Cloning, expression and immunolocalization pattern of a cinnamyl dehydrogenase gene from strawberry (*Fragaria × ananassa* cv. Chandler). *J Exp Bot* 375: 1723-34
- Bradford MM (1976) A rapid and sensitive method for the quantitation of microgram quantities of protein utilizing the principle of protein-dye binding. *Anal Biochem* 72: 248-254
- Brandelli A, Lopes CHGL (2005) Polyphenoloxidase activity, browning potential and phenolics content of peaches during postharvest ripening. *J Food Biochem* 29: 624-637
- Bravo L (1998) Polyphenols: Chemistry, dietary sources, metabolism, and nutritional significance. *Nutr Rev* 56: 317-333
- Brovelli EA, Brecht JK, Sherman WB, Sims CA (1999) Nonmelting-flesh trait in peaches is not related to low ethylene production rates. *HortScience* 34: 313-315
- Bunsiri A, Paull RE, Ketsa S (2012) Increased activities of phenylalanine ammonia lyase, peroxidase, and cinnamyl alcohol dehydrogenase in relation to pericarp hardening after physical impact in

- mangosteen (*Garcinia mangostana* L.). J Hortic Sci Biotech 87: 231-236
- Bureau S, Renard CMGC, Reich M, Ginies C, Audergon JM (2009) Change in anthocyanin concentrations in red apricot fruits during ripening. Food Sci Technol 42: 372-377
- Cai C, Xu CJ, Li X, Ferguson I, Chen K (2006a) Accumulation of lignin in relation to change in activities of lignification enzymes in loquat fruit flesh after harvest. Postharvest Biol Tec 40:163-169
- Cai C, Xu CJ, Shan LL, Li X, Zhou CH, Zhang WS, Ferguson I, Chen KS (2006b) Low temperature conditioning reduces postharvest chilling injury in loquat fruit. Postharvest Biol Tec 41: 252-259
- Concha CM, Figueroa NE, Poblete LA, Oñate FA, Schwab W, Figueroa CR (2013) Methyl jasmonate treatment induces changes in fruit ripening by modifying the expression of several ripening genes in *Fragaria chiloensis* fruit. Plant Physiol Biochem 70: 433-444
- Dangcham S, Ketsa S (2007) Relationship between maturity stages and low temperature involved in the pericarp hardening of mangosteen fruit after storage. Thai J Agr Sci 40: 143-150
- Dangcham S, Bowen J, Ferguson IB, Ketsa S (2008) Effect of temperature and low oxygen on pericarp hardening of mangosteen fruit stored at low temperature. Postharvest Biol Tec 50: 37-44
- Dardick CD, Callahan AM, Chiozzotto R, Schaffer RJ, Piagnani MC, Scorza R (2010) Stone formation in peach fruit exhibits spatial coordination of the lignin and flavonoid pathways and similarity to *Arabidopsis* dehiscence. BMC Biol 8: 13-30
- Deng WW, Zhang M, Wu JQ, Jiang ZZ, Tang L, Li YY, Wei CL, Jiang CJ, Wan XC (2013) Molecular cloning, functional analysis of three cinnamyl alcohol dehydrogenase (CAD) genes in the leaves of tea plant, *Camellia sinensis*. J Plant Physiol 170: 272-282
- de Pascual-Teresa S (2014) Molecular mechanisms involved in the cardiovascular and neuroprotective effects of anthocyanins. Arch Biochem Biophys 559:68-74
- Fuss E (2007), Biosynthesis of Lignans. Habilitationsschrif. Heinrich-Heine-Universität, Düsseldorf. http://docserv.uni-duesseldorf.de/servlets/DerivateServlet/Derivate-13524/Habilitationsschrift_Fuss.pdf
- Ghiani A, Negrini N, Morgutti S, Baldin F, Nocito FF, Spinardi A, Mignani I, Bassi D, Cocucci M (2011) Melting of 'Big Top' nectarine fruit: some physiological, biochemical, and molecular aspects. J Am Soc Hortic Sci 136: 61-68
- Goffner D, Doorsselaere JV, Yahiaoui N, Samaj J, Grima-Pettenati J, BouDET AM (1998) A novel aromatic alcohol dehydrogenase in higher plants: molecular cloning and expression. Plant Mol Biol 36: 755-765
- Hayama H, Ito A, Moriguchi T, Kashimura Y (2003) Identification of a new expansin gene closely associated with peach fruit softening. Postharvest Biol Tec 29: 1-10
- Iglesias I, Carbó J (2009) Melocoton plano y nectarina plana: las variedades de más interés. Instituto de Investigación y Tecnología Agroalimentarias (IRTA), Barcelona, Spain, pp 134 (in Spanish).

- Jaakola L (2013) New insights into the regulation of anthocyanin biosynthesis in fruits. *Trends Plant Sci* 18: 477-483
- Kao MWS, Brecht JK, Williamson JG, Huber DJ (2012) Ripening development and quality of Melting and Non-melting Flesh peach cultivars. *HortScience* 47: 879-885
- Kim JI, Ciesielski PN, Donohoe BS, Chapple C, Li X (2014) Chemically induced conditional rescue of the *Reduced Epidermal Fluorescence8* mutant of *Arabidopsis* reveals rapid restoration of growth and selective turnover of secondary metabolite pools. *Plant Physiol* 164: 584-595
- Kim SJ, Kim MR, Bedgar DL, Moinuddin SGA, Cardenas CL, Davin LB, Kang CL, Lewis NG (2004) Functional reclassification of the putative cinnamyl alcohol dehydrogenase multigene family in *Arabidopsis*. *Proc Natl Acad Sci USA* 101: 1455-1460
- Kirch H-H, Bartels D, Wei Y, Schnable PS, Wood AJ (2004) The ALDH gene superfamily of *Arabidopsis*. *Trends Plant Sci* 9: 371-377
- Laemmli UK (1970) Cleavage of structural proteins during the assembly of bacteriophage T4. *Nature* 227: 680-685
- Larkin MA, Blackshields G, Brown NP, Chenna R, McGgettigan PA, McWilliam H, Valentin F, Wallace IM, Wilm A, Lopez R, Thompson JD, Gibson TJ, Higgins DG (2007) Clustal W. Clustal X version 2.0. *Bioinformatics* 23: 2947-2948
- Lee J, Durst RW, Wrolstad RE (2005) Determination of total monomeric anthocyanin pigment content of fruit juices, beverages, natural colorants, and wines by the pH differential method: collaborative study. *J AOAC Int* 88: 1269-1278
- Legua P, Hernández F, Díaz-Mula HM, Valero D, Serrano M (2011) Quality, bioactive compounds and antioxidant activity of new flat-type peaches and nectarine cultivars: a comparative study. *J Food Sci* 76: C729-735
- Lester DR, Sherman WB, Atwell BJ (1996) Endopolygalacturonase and the melting flesh (M) locus in peach. *J Am Soc Hortic Sci* 121: 231-235
- Lewis NG, Yamamoto E (1990) Lignin: occurrence, biogenesis and biodegradation. *Annu Rev Plant Physiol Plant Mol Biol* 41: 455-496
- Li L, Ban ZJ, Li XH, Wu MY, Wang AL, Jiang YQ, Jiang YH (2012) Differential expression of anthocyanin biosynthetic genes and transcription factor *PcMYB10* in pears (*Pyrus communis* L.). *PLoS ONE* 7(9): e46070
- Lima GPP, Vianello F, Corrêa CR, da Silva Campos RA, Borguini MG (2014) Polyphenols in fruits and vegetables and its effect on human health. *Food Nutr Sci* 5: 1065-1082
- Lurie S, Friedman H, Weksler A, Dagar A, Eccher Zerbini P (2013) Maturity assessment at harvest and prediction of softening in an early and late season melting peach. *Postharvest Biol Tec* 76: 10-16
- Mansell RL, Gross C, Stockigt J, Franke H, Zenk MH (1974) Purification and properties of cinnamyl

- alcohol dehydrogenase from higher plants involved in lignin biosynthesis. *Phytochemistry* 13: 2427-2437
- McGuire R G (1992) Reporting of objective colour measurements. *HortScience* 27: 1254-1255
- Mita S, Kawamura S, Yamawaki K, Nakamura K, Hyodo H (1998) Differential expression of genes involved in the biosynthesis and perception of ethylene during ripening of passion fruit (*Passiflora edulis* Sims). *Plant Cell Physiol* 39: 1209-1217
- Mita S, Nagai Y, Asai T (2006) Isolation of cDNA clones corresponding to genes differentially expressed in pericarp of mume (*Prunus mume*) in response to ripening, ethylene and wounding signals. *Physiol Plant* 128: 531-545
- Monet R, Bassi, D (2008) 3 Classical Genetics and Breeding. In: Layne DR, Bassi D (eds) *The Peach - Botany, Production and Uses*, CAB International, Wallingford, pp 61-84
- Morgutti S, Negrini N, Mignani I, Bassi D, Cocucci M (2005) Flesh softening and phosphorylation of soluble polypeptides in relation to ethylene production in *Prunus persica* fruits with different ripening patterns. *Acta Hortic* 682: 155-162
- Morgutti S, Negrini N, Nocito FF, Ghiani A, Bassi D, Cocucci M (2006) Changes in endopolygalacturonase levels and characterization of a putative *endoPG* gene during fruit softening in peach genotypes with nonmelting and melting flesh fruit phenotypes. *New Phytol* 171: 315-328
- Nair RB, Bastress KL, Ruegger MO, Denault JW, Chapple C (2004) The *Arabidopsis thaliana REDUCED EPIDERMAL FLUORESCENCE1* gene encodes an aldehyde dehydrogenase involved in ferulic acid and sinapic acid biosynthesis. *Plant Cell* 16: 544-554
- Nakatsuka A, Shiomi S, Kubo Y, Inaba A (1997) Expression and internal feedback regulation of ACC synthase and ACC oxidase genes in ripening tomato fruit. *Plant Cell Physiol* 38: 1103-1110
- O'Malley DM, Porter S, Sederoff RR (1992) Purification, characterization, and cloning of cinnamyl alcohol dehydrogenase in loblolly pine (*Pinus taeda* L.). *Plant Physiol* 98: 1364-1371
- Peace CP, Crisosto CH, Gradziel TM (2005) Endopolygalacturonase: a candidate gene for freestone and melting flesh in peach. *Mol Breeding* 16: 21-31
- Prinsi B, Negri AS, Fedeli C, Morgutti S, Negrini N, Cocucci M, Espen L (2011) Peach fruit ripening: a proteomic comparative analysis of the mesocarp of two cultivars with different flesh firmness at two ripening stages. *Phytochemistry* 72: 1251-1262
- Ralph J (2010) Hydroxycinnamates in lignification. *Phytochem Rev* 9: 65-83
- Ring L, Yeh SY, Hücherig S, Hoffmann T, Blanco-Portales R, Fouche M, Villatoro C, Denoyes B, Monfort A, Caballero JL, Muñoz-Blanco J, Gershenson J, Schwab W (2013) Metabolic interaction between anthocyanin and lignin biosynthesis is associated with peroxidase FaPRX27 in strawberry fruit. *Plant Physiol* 163: 43-60
- Robertson JA, Horvat RJ, Lyon BG, Meredith FI, Senter S, Okie WR (1990) Comparison of quality

- characteristics of selected yellow- and white-fleshed peach cultivars. *J Food Sci* 55: 1308-1311
- Rozen S, Skaletsky HJ (2000) Primer3 on the WWW for general users and for biologist programmers. In: Krawetz S, Misener S (eds) *Bioinformatics Methods and Protocols: Methods in Molecular Biology*. Humana Press, Totowa, pp 365-386
- Rubinstein ND, Mayrose I, Martz E, Pupko T (2009) Epitopia: a web-server for predicting B-cell epitopes. *BMC Bioinformatics* 10: 287
- Saballos A, Ejeta G, Sanchez E, Kang C, Vermeris W (2009) A genomewide analysis of the cinnamyl alcohol dehydrogenase family in sorghum [*Sorghum bicolor* (L.) Moench] identifies *SbCAD2* as the *brown midrib6* gene. *Genetics* 181: 783-795
- Saitou N, Nei M (1987) The neighbor-joining method: a new method for reconstruction phylogenetic trees. *Mol Biol Evol* 4: 406-425
- Salentijn EMJ, Aharoni A, Schaart JG, Boone MJ, Krens FA (2003) Differential gene expression analysis of strawberry cultivars that differ in fruit firmness. *Physiol Plant* 118: 571-578
- Scalbert A, Monties B, Janin G (1989) Tannins in wood: comparison of different estimation methods. *J Agric Food Chem* 37, 1324-1329
- Schägger H, von Jagow G (1987) Tricine-sodium dodecyl sulfate-polyacrylamide gel electrophoresis for the separation of proteins in the range from 1 to 100 kDa. *Anal Biochem* 166, 368-379
- Seymour GB, Taylor JE, Tucker GA (eds) (1993) *Biochemistry of fruit ripening*. Chapman and Hall, London and New York
- Shan L, Li X, Wang P, Cai C, Zhang B, Sun C, Zhang W, Xu C, Ferguson I, Chen K (2008) Characterization of cDNAs associated with lignification and their expression profiles in loquat fruit with different lignin accumulation. *Planta* 227: 1243-1254
- Shen Z, Confolent C, Lambert P, Poëssel JL, Quilot-Turion B, Yu M, Ma R, Pascal T (2013) Characterization and genetic mapping of a new blood-flesh trait controlled by the single dominant locus DBF in peach. *Tree Genet Genomes* 9: 1435-1446
- Sherman BW, Topp BL, Lyrene PM (1990) Non-melting flesh for fresh market peaches. *Proc Fla State Hort Soc* 103: 293-294
- Shinya P, Contador L, Predieri S, Rubio P, Infante R (2013) Peach ripening: segregation at harvest and postharvest flesh softening. *Postharvest Biol Tec* 86: 472-478
- Sibout R, Eudes A, Pollet B, Goujon T, Mila I, Granier F, Séguin A, Lapierre C, Jouanin L (2003) Expression pattern of two paralogs encoding cinnamyl alcohol dehydrogenases in *Arabidopsis*. Isolation and characterization of the corresponding mutants. *Plant Physiol* 132: 848-860
- Sloan E (2008) Top 10 functional food trends. *Food Technol* 62: 24-44.
- Strommer J (2011) The plant ADH gene family. *Plant J* 66: 128-142
- Tamura K, Dudley J, Nei M, Kumar S (2007) MEGA4: molecular evolutionary genetics analysis (MEGA) software version 4.0. *Mol Biol Evol* 24: 1596-1599
- Thévenin J, Pollet B, Letarnec B, Saulnier L, Gissot L, Maia-Grondard A, Lapierre C, Jouanin L

- (2011) The simultaneous repression of CCR and CAD, two enzymes of the lignin biosynthetic pathway, results in sterility and dwarfism in *Arabidopsis thaliana*. Mol Plant 4: 70-82
- Tobias CM, Chow EK (2005) Structure of the cinnamyl-alcohol dehydrogenase gene family in rice and promoter activity of a member associated with lignification. Planta 220: 678-688
- Tomás-Barberan FA, Ferreres F, Gil MI (2000) Antioxidant phenolic metabolites from fruit and vegetables and changes during postharvest storage and processing. In: Rahman A (ed) Studies in Natural Products Chemistry, Part D. Elsevier Science, Amsterdam, 23: 739-795
- Tong Z, Qu S, Zhang J, Wang F, Tao J, Gao Z, Zhang Z (2012) A modified protocol for RNA extraction from different peach tissues suitable for gene isolation and Real-Time PCR analysis. Mol Biotechnol 50: 229-236
- Tonutti P, Casson PC, Ramina A (1991) Ethylene biosynthesis during peach fruit development. J Am Soc Hortic Sci 116: 274-279
- Tonutti P, Bonghi C, Ramina A (1996) Fruit firmness and ethylene biosynthesis in three cultivars of peach (*Prunus persica* L. Batsch). J. Hortic Sci 71: 141-147
- Tonutti P, Bonghi C, Ruperti B, Tornielli GB, Ramina A (1997) Ethylene evolution and 1-aminocyclopropane-1-carboxylate oxidase gene expression during early development and ripening of peach fruit. J Am Soc Hortic Sci 122: 642-647
- Umesh S, Kavitha R (2011) Induction of cinnamyl alcohol dehydrogenase in bacterial spot disease resistance of tomato. J Bacteriol Rev 3: 16-27
- van der Rest B, Dannoun S, Boudet AM, Rochange SF (2006) Down-regulation of cinnamoyl-CoA reductase in tomato (*Solanum lycopersicum* L.) induces dramatic changes in soluble phenolic pools. J Exp Bot 57: 1399-1411
- Vanholme R, Demedts B, Morreel K, Ralph J, Boerjan W (2010) Lignin biosynthesis and structure. Plant Physiol 153: 895-905
- Vanholme R, Morreel K, Darrah C, Oyarce P, Grabber JH, Ralph J, Boerjan W (2012) Metabolic engineering of novel lignin in biomass crops. New Phytol 196: 978-1000
- Vauzour D, Rodriguez-Mateos A, Corona G, Oruna-Concha MJ, Spencer JPE (2010) Polyphenols and human health: prevention of disease and mechanisms of action. Nutrients 2: 1106-1131
- Verde I, Abbott AG, Scalabrin S, Jung S, Su S, Marroni F, Zhebentyayeva T, Dettori MT, Grimwood J, Cattonaro F, Zuccolo A, Rossini L, Jenkins J, Meisel LA, Decroocq V, Sosinski B, Prochnik S, Mitros T, Policriti A, Cipriani G, Dondini L, Ficklin S, Goodstein DM, Xuan P, Del Fabbro C, Aramini V, Copetti D, Gonzalez S, Horner DS, Falchi R, Lucas S, Mica E, Maldonado J, Lazzari B, Bielenberg D, Pirona R, Miculan M, Barakat A, Testolin R, Stella A, Tartarini S, Tonutti P, Arús P, Orellana A, Wells C, Main D, Vizzotto G, Silva H, Salamini F, Schmutz J, Morgante M, Rokhsar DS (2013) The high-quality draft genome of peach (*Prunus persica*) identifies unique patterns of genetic diversity, domestication and genome evolution. Nat Genet 45: 487-494
- Ververidis P, Trantas E, Douglas C, Vollmer G, Kretzschmar G, Panopoulos N (2007) Biotechnology

- of flavonoids and other phenylpropanoid-derived natural products. Part I: Chemical diversity, impacts on plant biology and human health. *Biotechnol J* 2: 1214-1234
- Waldron KW, Smith AC, Parr AJ, Ng A, Parker ML (1997) New approaches to understanding and controlling cell separation in relation to fruit and vegetable texture. *Trends Food Sci Tech* 8: 213-221
- Wang SY, Chen C, Wang CY (2009) The influence of light and maturity on fruit quality and flavonoid content of red raspberries. *Food Chem* 112: 676-684
- Zhong CX, Ikoma Y, Yano M, Ogawa K, Hyodo H (1998) Varietal differences in the potential to produce ethylene and gene expression of ACC synthase and ACC oxidase between 'Kui mi' and 'Hong xin' of Chinese kiwifruit. *J Jpn Soc Hortic Sci* 67: 204-209

Supporting information

Additional Supporting Information may be found in the online version of this article:

Appendix S1. Table 1. Sequences of the PCR primers used (Primer3 web resource; <http://bioinfo.ut.ee/primer3/>).

Appendix S2. Figure 1. Alignment of the 24 deduced PRUPE_CAD proteins of *P. persica* and reciprocal identity scores.

Appendix S3. Table 2: Identity scores of the 24 deduced PRUPE_CAD proteins of *P. persica* against strawberry FaCAD.

Appendix S4. Table 3: Deduced molecular weights (Mw) and pIs of the putative *P. persica* PRUPE_CAD proteins.

Figure legends

Fig. 1. Visual appearance of NMF ‘Oro A’ (A), MF ‘Springcrest’ (B) and MF ‘Sanguinella’ (C) peach fruit at S4 III ripening stage (white bar: 4 cm); colour index a* (D) and fresh weight (E) of NMF ‘Oro A’, MF ‘Springcrest’ and MF ‘Sanguinella’ peach fruit at three (S3, S4 I and S4 III) ripening stages. S3, S4 I and S4 III stages corresponded respectively to: ‘Oro A’, 98, 101 and 104 DAFB; ‘Springcrest’, 70, 84 and 97 DAFB; ‘Sanguinella’, 138, 147 and 154 DAFB. For colour index a*, the results are presented as means \pm SE of measurements on at least eight fruits from five different plants per each genotype (n=40); for fruit growth, the results are means \pm SE of measurements on at least five fruits from five different plants per each genotype (n=25). Different letters indicate significant differences ($P<0.05$). Lower case letters refer to differences among ripening stages within each genotype; capital letters refer to differences among genotypes at the same ripening stage.

Fig. 2. Ethylene emission by NMF ‘Oro A’, MF ‘Springcrest’ and MF ‘Sanguinella’ peach fruit at three ripening stages. Results are presented as means \pm SE of measurements on at least three fruits from five different plants per each genotype (n=15). ND: not detectable. Different letters indicate significant differences ($P<0.05$). Lower case letters refer to differences among ripening stages within each genotype; capital letters refer to differences among genotypes at the same ripening stage.

Fig. 3. Fruit firmness (A) and total soluble solids (SSC; B) in ‘NMF ‘Oro A’, MF ‘Springcrest’ and MF ‘Sanguinella’ peach fruit at three ripening stages. Results are presented as means \pm SE of measurements on at least five fruits from five different plants per each genotype (n=25). Different letters indicate significant differences ($P<0.05$). Lower case letters refer to differences among ripening stages within each genotype; capital letters refer to differences among genotypes at the same ripening stage.

Fig. 4. Total phenolics (A), anthocyanins (B) and lignin (C) contents in NMF ‘Oro A’, MF ‘Springcrest’ and MF ‘Sanguinella’ peach fruit at three ripening stages. Results are presented as means \pm SE of two measurements from two separate extractions (n=4). ND: not detectable. Different letters indicate significant differences ($P<0.05$). Lower case letters refer to differences among ripening stages within each genotype; capital letters refer to differences among genotypes at the same ripening stage.

Fig. 5. In vitro (‘bulk’) CAD activity in the mesocarp of NMF ‘Oro A’, MF ‘Springcrest’ and MF ‘Sanguinella’ peach fruit at three ripening stages. Results are presented as means \pm SE of three measurements from two separate extractions (n=6). ND: not detectable. Different letters indicate significant differences ($P<0.05$). Lower case letters refer to differences among ripening stages within each genotype; capital letters refer to differences among genotypes at the same ripening stage.

Fig. 6. Phylogenetic relationship analysis of the 24 putative full-length PRUPE_CAD sequences and their grouping on the basis of proposed functional class (Deng et al. 2013). Clustal W 2.1 was used for

the alignment of sequences and the tree was constructed using Neighbor-joining method with MEGA4; each interior branch represents the percentage of bootstrap value (1000 replicates), and only those $\geq 50\%$ are indicated by numbers. Amino acid sequences were retrieved from NCBI and Phytozome databases and their accession numbers are noted. The phylogenetic tree includes the following plant species: *Arabidopsis thaliana* (AtCAD1-AtCAD12); *Aralia cordata* (AcCAD); *Artemisia annua* (AaCAD); *Camellia sinensis* (CsCAD1-CsCAD3); *Capsicum annum* (CaCAD); *Eriobotrya japonica* (EjCAD1); *Eucalyptus botryoides* (EbCAD); *Eucalyptus gunnii* (EgCAD); *Fragaria × ananassa* (FaCAD), *Gossypium hirsutum* (GhCAD1 and GhCAD6); *Leucaena leucocephala* (LlCAD); *Lolium perenne* (LpCAD); *Medicago sativa* (MsCAD1 and MsCAD2); *Nicotiana tabacum* (NtCAD1); *Oryza sativa* (OsCAD2); *Petroselinum crispum* (PcCAD); *Populus tremuloides* (PtCAD); *Prunus mume* (PmCAD); *Prunus persica* (PRUPE_CADs); *Quercus suber* (QsCAD); *Saccharum officinarum* (SoCAD); *Triticum aestivum* (TaCAD). PRUPE_CAD isoforms are identified by numbers of the scaffold (sc) where the encoding gene sequences are located.

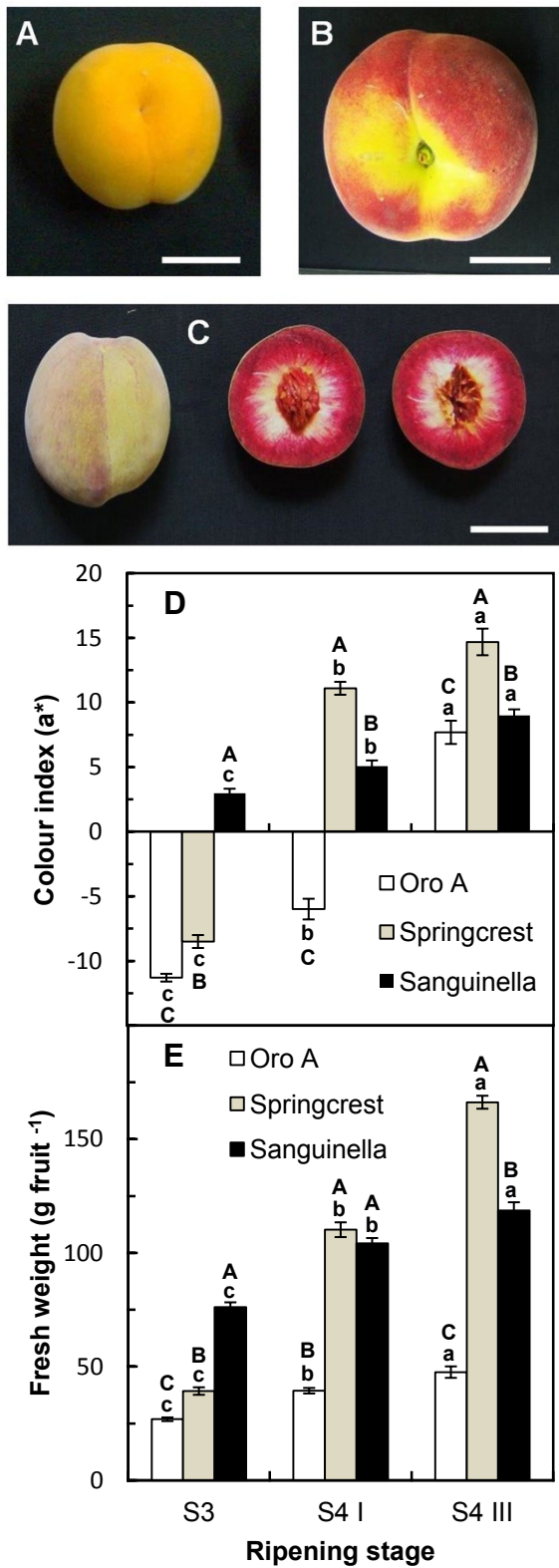
Fig 7. Alignment of amino acid sequences of putative PRUPE_CAD sc6₅ (GenBank accession PRUPE_ppa007622m) and PRUPE_CAD sc8₂ (PRUPE_ppa007736m) with CADs from other plant species. FaCAD, *F. × ananassa* (AAK28509.1); EjCAD1, *E. japonica* (ABV44810.1); PmCAD, *P. mume* (BAE48658.1); AtCAD4 and AtCAD5, *A. thaliana* (AAP59434.1 and AAP59435.1, respectively); CsCAD2, *C. sinensis* (ADO51749.1). Sequences of Zn1, Zn2 and coenzyme binding motifs are shown in boxes; the conserved amino acids in these binding motifs are evidenced in gray. In bold, underlined characters is indicated the PRUPE_CAD sc8₂ immunogenic 15-amino acid sequence (positions 114-128) used for the development of specific polyclonal antibodies.

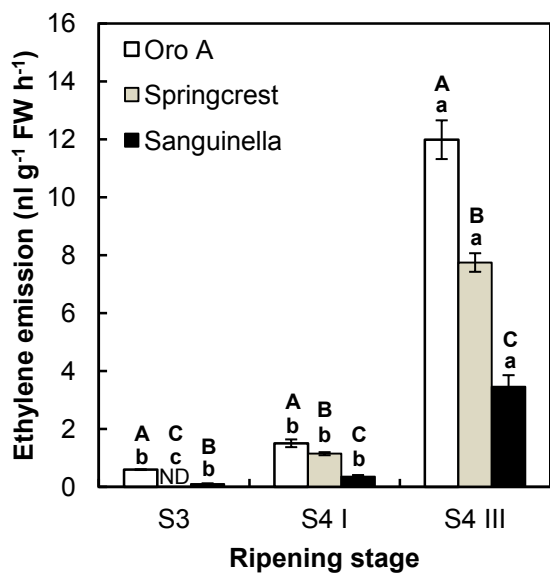
Fig. 8. Levels of putative CAD (PRUPE_CAD sc6 and PRUPE_CAD sc8) isoforms in the mesocarp of NMF ‘Oro A’, MF ‘Springcrest’ and MF ‘Sanguinella’ peach fruit at three ripening stages. Immunoblotting of PRUPE_CAD polypeptides after SDS-PAGE. Loading (10 μ g protein per lane) was equal in all lanes; the results of one experiment, representative of three, are shown. Upper panel: probing with anti-FaCAD polyclonal antibodies; lower panel: probing with anti-PRUPE_CAD sc8 polyclonal antibodies.

Fig. 9. In gel CAD activity and levels of PRUPE_CAD sc6 and PRUPE_CAD sc8 isoforms in NMF ‘Oro A’, MF ‘Springcrest’ and MF ‘Sanguinella’ peach fruit at three ripening stages. Activity staining (uppermost panel) and immunoblotting of PRUPE_CAD proteins with anti-FaCAD (PRUPE_CAD sc6) and anti-PRUPE_CAD sc8 (PRUPE_CAD sc8) polyclonal antibodies (lower panels) were conducted after native-PAGE of mesocarp soluble proteins. Loading (10 μ g protein per lane) was equal in all lanes; the results of one experiment, representative of three, are shown.

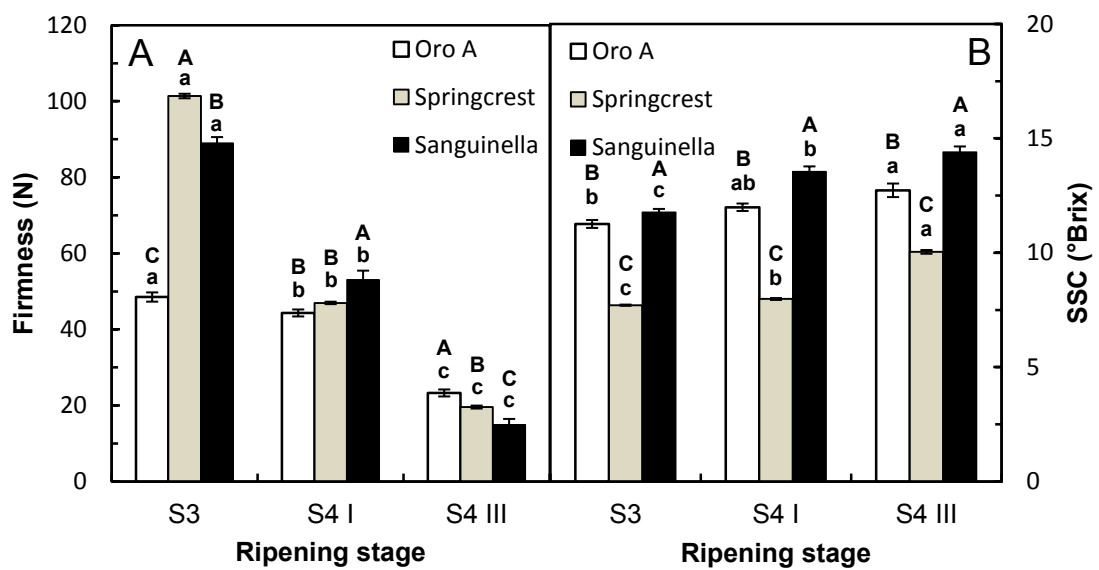
Fig. 10. Semi-quantitative gene expression analysis of *PRUPE_CAD sc6₁₋₅* (*PRUPE_ppa007622mg*,

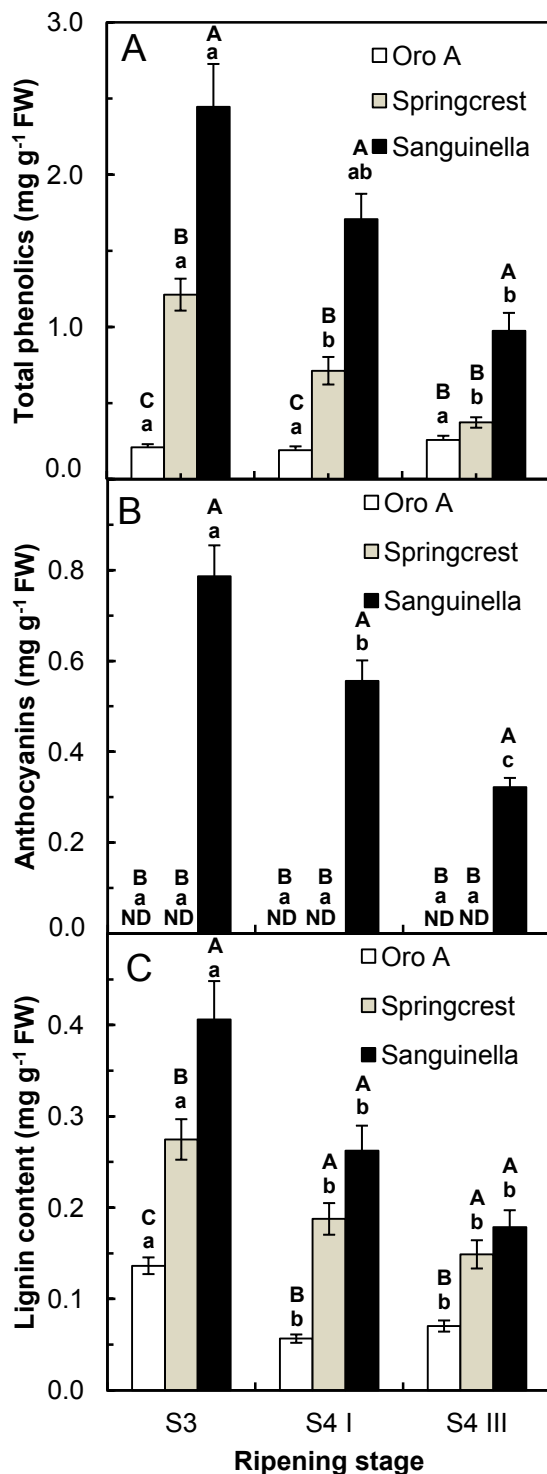
PRUPE_ppa007613mg, *PRUPE_ppa007226mg*, *PRUPE_ppa016455mg*, *PRUPE_ppa007668mg*), *PRUPE_CAD_sc8_{1,2}* (*PRUPE_ppa007749mg* and *PRUPE_ppa007636mg*) and *PRUPE_ACO1* (*PRUPE_ppa008791mg*) genes in NMF ‘Oro A’, MF ‘Springcrest’ and MF ‘Sanguinella’ peach fruit at three ripening stages. Primer sequences are reported in Appendix S1 in Supporting Information. A ribosomal *PRUPE_S16* (*PRUPE_ppa012996mg*) gene was used as internal control. Gel images refer to one experiment representative of three.

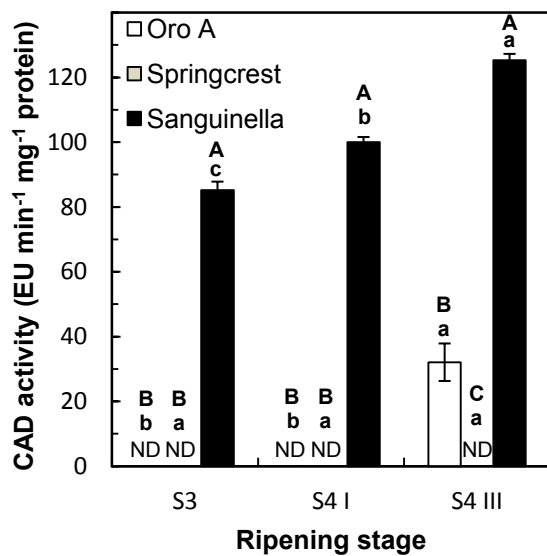


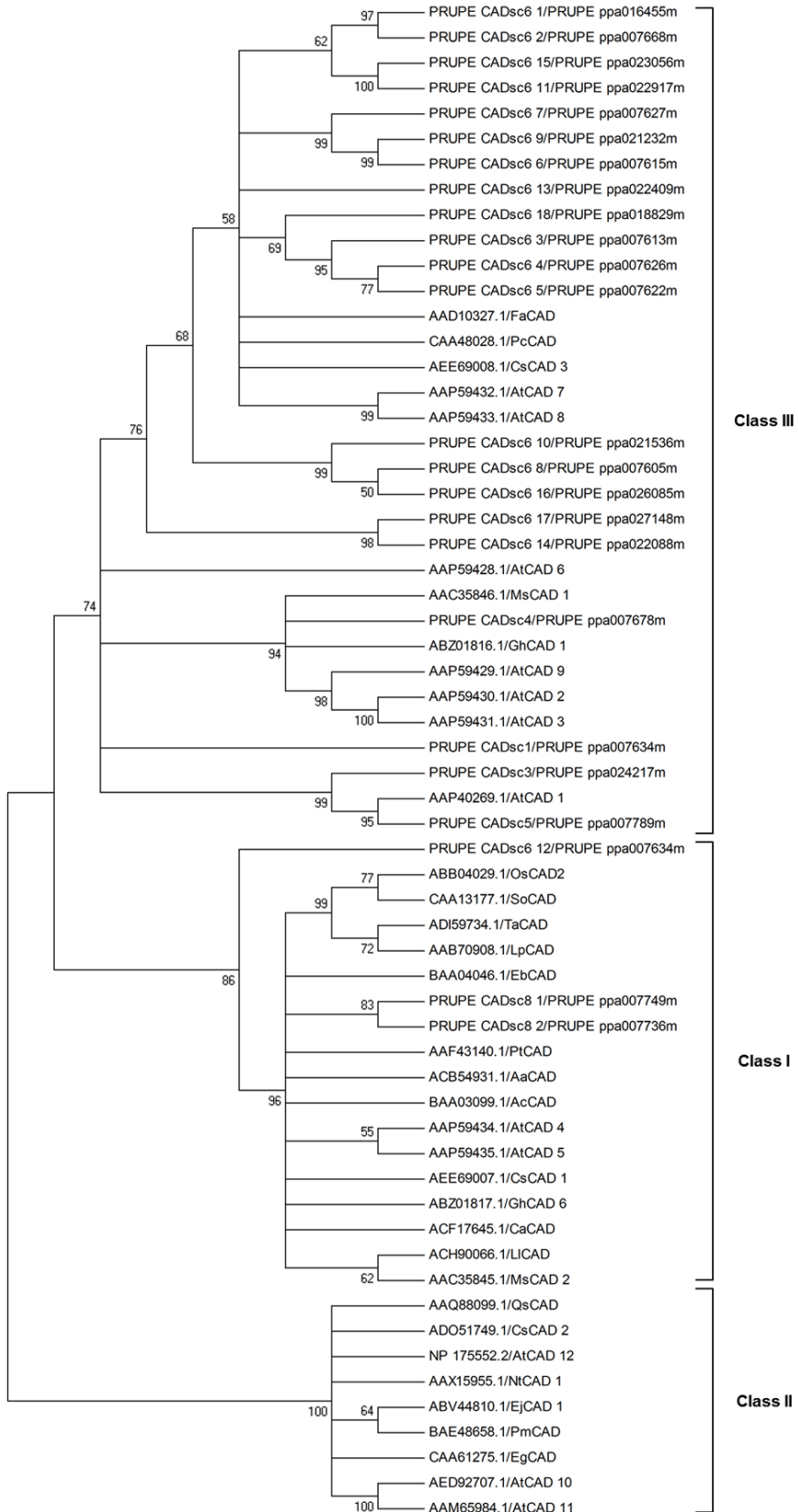


a









Gabotti et al. "Cinnamyl alcohol dehydrogenase.." Fig. 6

FaCAD_AAK28509.1	--MS IEQEHPNKASGWAARDSSGVLSFPNF SRRETGEKDMFKVL YCGICHSDHHMVKNE	58
CADsc6s_PRUPE_pp=007622m	MVVSTIEQEHFHKAFGWAARDSSGVLSFPKFSSRRETGEKDVLFKVL YCGICHSDLHMVKNE	60
CADsc8s_PRUPE_pp=007736m	--MGSLE-VERTTGWAARDSSGILSPYTYLRLNTG PEDVYKVVLSCGICHSDLHQVKND	57
EjCAD1_ABV44810.1	-----	0
PmCAD_BAE48658.1	-----	0
AtCAD4_AAP59434.1	--MG SVEAGERKALGWAARDPSGVLSPLSPSYTLRSTGADDVYIKVICCGICHTDIHQIKND	58
AtCAD5_AAP59435.1	--MG IME-AERKTTGWAARDPSGLILSPYTYTLRETGPDVNIRIICCGICHTDLHQTRND	57
CsCAD2_ADO51749.1	-----	0
Zn1 binding motif		
WGFSTYPLVHE	IIGEVIEVESPQSKVQKFKVQGDRGVGCVIGS	118
CADsc6s_PRUPE_pp=007622m	GSRSCCENCTDHLENYC	118
CADsc8s_PRUPE_pp=007736m	PKQ	120
EjCAD1_ABV44810.1	WGSSTYPLVHE	117
PmCAD_BAE48658.1	GHEVIEVESPQSKVQKFKVQGDRGVGCVIGS	0
AtCAD4_AAP59434.1	GCHSCSDBCANNLENVCPKM	13
AtCAD5_AAP59435.1	LGRSNYPMVPHE	118
CsCAD2_ADO51749.1	VVSVLVEVGSDF	117
FaCAD_AAK28509.1	-----	12
CADsc6s_PRUPE_pp=007622m	--MSGAGKV-----	13
CADsc8s_PRUPE_pp=007736m	VCVIG-----	118
EjCAD1_ABV44810.1	LGMSNYPMVPHE	117
PmCAD_BAE48658.1	VVSVLVEVESPQSKVQKFKVQGDRGVGCVIGS	118
AtCAD4_AAP59434.1	GCHSCSDBCANNLENVCPKM	0
AtCAD5_AAP59435.1	LGMSNYPMVPHE	117
CsCAD2_ADO51749.1	VVSVLVEVESPQSKVQKFKVQGDRGVGCVIGS	12
FaCAD_AAK28509.1	-----	178
CADsc6s_PRUPE_pp=007622m	ILTYGANYYDGTTTYYGGCS	178
CADsc8s_PRUPE_pp=007736m	DIMVAHEHFFVVRIPDNLPLDGAAPLLCAGITTYSPRLYFGL	180
EjCAD1_ABV44810.1	ILTYGSKYLDGTTTYGGYSDIMVADEHFIVRVD3SLPLDGAAPLLCAGITTYSPRLYFGL	177
PmCAD_BAE48658.1	IWSYNDTYSQDGKFTQGGFAFELVADQKFVVKIPDGMAWQAAPLLCA	12
AtCAD4_AAP59434.1	GAGVTVYSPLSHFG	32
AtCAD5_AAP59435.1	WVRLLLLQRGYT-----	178
CsCAD2_ADO51749.1	IWSYNDVYITDGKFTQGGFAFADTMVNQKFVVKIPEGM	177
FaCAD_AAK28509.1	VAPEQAAPLLCA	31
CADsc6s_PRUPE_pp=007622m	GAGVTVYSPLSHFG	31
CADsc8s_PRUPE_pp=007736m	WVRLLLLQRGYT-----	31
EjCAD1_ABV44810.1	-----	31
PmCAD_BAE48658.1	ASGYIA3WLVKKLQLQRGYT-----	31
AtCAD4_AAP59434.1	-----	31
AtCAD5_AAP59435.1	-----	31
CsCAD2_ADO51749.1	-----	31
NADPH binding motif		
DRPGMHVGVVHE	HVAVKFAKAMGVKVVIV1ST5PKREEE-ALEHLGADSF	237
CADsc6s_PRUPE_pp=007622m	FLV5RQDQ	239
CADsc8s_PRUPE_pp=007736m	DRPGMHVGVVHE	236
EjCAD1_ABV44810.1	HVAVKFAKAMGVKVVIV1ST5PKREEE-AIDHLHADSF	45
PmCAD_BAE48658.1	FLV5RQDQ	65
AtCAD4_AAP59434.1	-----	237
AtCAD5_AAP59435.1	AKA SIRD PNDPFTK EHLHALDEAQDLQLFKAN	236
CsCAD2_ADO51749.1	-----	64
FaCAD_AAK28509.1	-----	237
CADsc6s_PRUPE_pp=007622m	NLSGLRRGGILS	239
CADsc8s_PRUPE_pp=007736m	GLGGVGHMGVVIKAMGHHVTVI	236
EjCAD1_ABV44810.1	SSDRKKEE-ALEHVGADEFLVSSDAT	12
PmCAD_BAE48658.1	-----	32
AtCAD4_AAP59434.1	-----	178
AtCAD5_AAP59435.1	IWSYNDVYINGQFTQGGFAKATVHVHQKFVVKIPEGM	177
CsCAD2_ADO51749.1	VAPEQAAPLLCA	31
FaCAD_AAK28509.1	-----	31
CADsc6s_PRUPE_pp=007622m	MASGLKGII	237
CADsc8s_PRUPE_pp=007736m	GLGGVGHMGVVIKAMGHHVTVI	236
EjCAD1_ABV44810.1	SSDRKKEE-AIEHLGADDVVSSDA	236
PmCAD_BAE48658.1	KQFGLRGGII	64
AtCAD4_AAP59434.1	-----	237
AtCAD5_AAP59435.1	-----	236
CsCAD2_ADO51749.1	-----	236
FaCAD_AAK28509.1	-----	286
CADsc6s_PRUPE_pp=007622m	HMQAAIGTMDGIIDT-VSAQHPPLPLGILK-----	286
CADsc8s_PRUPE_pp=007736m	SHGKLVVMVGAPEKPLELPV	288
EjCAD1_ABV44810.1	QMQAAIGTMDGIIDT-VSAVHPPLPLGILK-----	288
PmCAD_BAE48658.1	SHGKLVVMVGAPEKPLELPV	285
AtCAD4_AAP59434.1	KMQEAADS LDYIIDT-VSAVHPPLPELYPSLRL-----	285
AtCAD5_AAP59435.1	LDGKLILMGVIGAPLQFVS	102
CsCAD2_ADO51749.1	LL--EEGSFDSAVERGEGV FHTA3FYHDVTDPAELLEPAVKGTLNVLNSCAKSFSIK-----	122
FaCAD_AAK28509.1	-----	122
CADsc6s_PRUPE_pp=007622m	LL--EEGSFDSAVERGEGV FHTA3FYHDVTDPAELLEPAVKGTLNVLNSCAKSFSIK-----	286
CADsc8s_PRUPE_pp=007736m	EMQRLADS LDYIIDT-VFVFHPLDFVLACLK-----	286
EjCAD1_ABV44810.1	LDGKLILMGVINTPLQFVT	285
PmCAD_BAE48658.1	KMSELADS LDVYIDT-VPVHHALEPYLSLLK-----	122
AtCAD4_AAP59434.1	-----	169
AtCAD5_AAP59435.1	LDGKLILMGVINNPLQFLT	169
CsCAD2_ADO51749.1	LL--EEGCFDSLVLVGDCEGV FHTA3FYHDVDPQVVELIDPAKGTLNVLGSCARNPSVK-----	121
FaCAD_AAK28509.1	-----	121
CADsc6s_PRUPE_pp=007622m	-----	238
CADsc8s_PRUPE_pp=007736m	-----	340
EjCAD1_ABV44810.1	-----	340
PmCAD_BAE48658.1	-----	340
AtCAD4_AAP59434.1	-----	340
AtCAD5_AAP59435.1	-----	340
CsCAD2_ADO51749.1	-----	340
FaCAD_AAK28509.1	-----	340
CADsc6s_PRUPE_pp=007622m	-----	340
CADsc8s_PRUPE_pp=007736m	-----	340
EjCAD1_ABV44810.1	-----	340
PmCAD_BAE48658.1	-----	340
AtCAD4_AAP59434.1	-----	340
AtCAD5_AAP59435.1	-----	340
CsCAD2_ADO51749.1	-----	340
FaCAD_AAK28509.1	-----	340
CADsc6s_PRUPE_pp=007622m	-----	340
CADsc8s_PRUPE_pp=007736m	-----	340
EjCAD1_ABV44810.1	-----	340
PmCAD_BAE48658.1	-----	340
AtCAD4_AAP59434.1	-----	340
AtCAD5_AAP59435.1	-----	340
CsCAD2_ADO51749.1	-----	340
FaCAD_AAK28509.1	-----	340
CADsc6s_PRUPE_pp=007622m	-----	340
CADsc8s_PRUPE_pp=007736m	-----	340
EjCAD1_ABV44810.1	-----	340
PmCAD_BAE48658.1	-----	340
AtCAD4_AAP59434.1	-----	340
AtCAD5_AAP59435.1	-----	340
CsCAD2_ADO51749.1	-----	340
FaCAD_AAK28509.1	-----	340
CADsc6s_PRUPE_pp=007622m	-----	340
CADsc8s_PRUPE_pp=007736m	-----	340
EjCAD1_ABV44810.1	-----	340
PmCAD_BAE48658.1	-----	340
AtCAD4_AAP59434.1	-----	340
AtCAD5_AAP59435.1	-----	340
CsCAD2_ADO51749.1	-----	340
FaCAD_AAK28509.1	-----	340
CADsc6s_PRUPE_pp=007622m	-----	340
CADsc8s_PRUPE_pp=007736m	-----	340
EjCAD1_ABV44810.1	-----	340
PmCAD_BAE48658.1	-----	340
AtCAD4_AAP59434.1	-----	340
AtCAD5_AAP59435.1	-----	340
CsCAD2_ADO51749.1	-----	340
FaCAD_AAK28509.1	-----	340
CADsc6s_PRUPE_pp=007622m	-----	340
CADsc8s_PRUPE_pp=007736m	-----	340
EjCAD1_ABV44810.1	-----	340
PmCAD_BAE48658.1	-----	340
AtCAD4_AAP59434.1	-----	340
AtCAD5_AAP59435.1	-----	340
CsCAD2_ADO51749.1	-----	340
FaCAD_AAK28509.1	-----	340
CADsc6s_PRUPE_pp=007622m	-----	340
CADsc8s_PRUPE_pp=007736m	-----	340
EjCAD1_ABV44810.1	-----	340
PmCAD_BAE48658.1	-----	340
AtCAD4_AAP59434.1	-----	340
AtCAD5_AAP59435.1	-----	340
CsCAD2_ADO51749.1	-----	340
FaCAD_AAK28509.1	-----	340
CADsc6s_PRUPE_pp=007622m	-----	340
CADsc8s_PRUPE_pp=007736m	-----	340
EjCAD1_ABV44810.1	-----	340
PmCAD_BAE48658.1	-----	340
AtCAD4_AAP59434.1	-----	340
AtCAD5_AAP59435.1	-----	340
CsCAD2_ADO51749.1	-----	340
FaCAD_AAK28509.1	-----	340
CADsc6s_PRUPE_pp=007622m	-----	340
CADsc8s_PRUPE_pp=007736m	-----	340
EjCAD1_ABV44810.1	-----	340
PmCAD_BAE48658.1	-----	340
AtCAD4_AAP59434.1	-----	340
AtCAD5_AAP59435.1	-----	340
CsCAD2_ADO51749.1	-----	340
FaCAD_AAK28509.1	-----	340
CADsc6s_PRUPE_pp=007622m	-----	340
CADsc8s_PRUPE_pp=007736m	-----	340
EjCAD1_ABV44810.1	-----	340
PmCAD_BAE48658.1	-----	340
AtCAD4_AAP59434.1	-----	340
AtCAD5_AAP59435.1	-----	340
CsCAD2_ADO51749.1	-----	340
FaCAD_AAK28509.1	-----	340
CADsc6s_PRUPE_pp=007622m	-----	340
CADsc8s_PRUPE_pp=007736m	-----	340
EjCAD1_ABV44810.1	-----	340
PmCAD_BAE48658.1	-----	340
AtCAD4_AAP59434.1	-----	340
AtCAD5_AAP59435.1	-----	340
CsCAD2_ADO51749.1	-----	340
FaCAD_AAK28509.1	-----	340
CADsc6s_PRUPE_pp=007622m	-----	340
CADsc8s_PRUPE_pp=007736m	-----	340
EjCAD1_ABV44810.1	-----	340
PmCAD_BAE48658.1	-----	340
AtCAD4_AAP59434.1	-----	340
AtCAD5_AAP59435.1	-----	340
CsCAD2_ADO51749.1	-----	340
FaCAD_AAK28509.1	-----	340
CADsc6s_PRUPE_pp=007622m	-----	340
CADsc8s_PRUPE_pp=007736m	-----	340
EjCAD1_ABV44810.1	-----	340
PmCAD_BAE48658.1	-----	340
AtCAD4_AAP59434.1	-----	340
AtCAD5_AAP59435.1	-----	340
CsCAD2_ADO51749.1	-----	340
FaCAD_AAK28509.1	-----	340
CADsc6s_PRUPE_pp=007622m	-----	340
CADsc8s_PRUPE_pp=007736m	-----	340
EjCAD1_ABV44810.1	-----	340
PmCAD_BAE48658.1	-----	340
AtCAD4_AAP59434.1	-----	340
AtCAD5_AAP59435.1	-----	340
CsCAD2_ADO51749.1	-----	340
FaCAD_AAK28509.1	-----	340
CADsc6s_PRUPE_pp=007622m	-----	340
CADsc8s_PRUPE_pp=007736m	-----	340
EjCAD1_ABV44810.1	-----	340
PmCAD_BAE48658.1	-----	340
AtCAD4_AAP59434.1	-----	340
AtCAD5_AAP59435.1	-----	340
CsCAD2_ADO51749.1	-----	340
FaCAD_AAK28509.1	-----	340
CADsc6s_PRUPE_pp=007622m	-----	340
CADsc8s_PRUPE_pp=007736m	-----	340
EjCAD1_ABV44810.1	-----	340
PmCAD_BAE48658.1	-----	340
AtCAD4_AAP59434.1	-----	340
AtCAD5_AAP59435.1	-----	340
CsCAD2_ADO51749.1	-----	340
FaCAD_AAK28509.1	-----	340
CADsc6s_PRUPE_pp=007622m	-----	340
CADsc8s_PRUPE_pp=007736m	-----	340
EjCAD1_ABV44810.1	-----	340
PmCAD_BAE48658.1	-----	340
AtCAD4_AAP59434.1	-----	340
AtCAD5_AAP59435.1	-----	340
CsCAD2_ADO51749.1	-----	340
FaCAD_AAK28509.1	-----	340
CADsc6s_PRUPE_pp=007622m	-----	340
CADsc8s_PRUPE_pp=007736m	-----	340
EjCAD1_ABV44810.1	-----	340
PmCAD_BAE48658.1	-----	340
AtCAD4_AAP59434.1	-----	340
AtCAD5_AAP59435.1	-----	340
CsCAD2_ADO51749.1	-----	340
FaCAD_AAK28509.1	-----	340
CADsc6s_PRUPE_pp=007622m	-----	340
CADsc8s_PRUPE_pp=007736m	-----	340
EjCAD1_ABV44810.1	-----	340
PmCAD_BAE48658.1	-----	340
AtCAD4_AAP59434.1	-----	340
AtCAD5_AAP59435.1	-----	340
CsCAD2_ADO51749.1	-----	340
FaCAD_AAK28509.1	-----	340
CADsc6s_PRUPE_pp=007622m	-----	340
CADsc8s_PRUPE_pp=007736m	-----	340
EjCAD1_ABV44810.1	-----	340
PmCAD_BAE48658.1	-----	340
AtCAD4_AAP59434.1	-----	340
AtCAD5_AAP59435.1	-----	340
CsCAD2_ADO51749.1	-----	340
FaCAD_AAK28509.1	-----	340
CADsc6s_PRUPE_pp=007622m	-----	340
CADsc8s_PRUPE_pp=007736m	-----	340
EjCAD1_ABV44810.1	-----	340
PmCAD_BAE48658.1	-----	340
AtCAD4_AAP59434.1	-----	340
AtCAD5_AAP59435.1	-----	340
CsCAD2_ADO51749.1	-----	340
FaCAD_AAK28509.1	-----	340
CADsc6s_PRUPE_pp=007622m	-----	340
CADsc8s_PRUPE_pp=007736m	-----	340
EjCAD1_ABV44810.1	-----	340
PmCAD_BAE48658.1	-----	340
AtCAD4_AAP59434.1	-----	340
AtCAD5_AAP59435.1	-----	340
CsCAD2_ADO51749.1	-----	340
FaCAD_AAK28509.1	-----	340
CADsc6s_PRUPE_pp=007622m	-----	340
CADsc8s_PRUPE_pp=007736m	-----	340
EjCAD1_ABV44810.1	-----	340
PmCAD_BAE48658.1	-----	340
AtCAD4_AAP59434.1	-----	340
AtCAD5_AAP59435.1	-----	340
CsCAD2_ADO51749.1	-----	340
FaCAD_AAK28509.1	-----	340
CADsc6s_PRUPE_pp=007622m	-----	340
CADsc8s_PRUPE_pp=007736m	-----	340
EjCAD1_ABV44810.1	-----	340
PmCAD_BAE48658.1	-----	340
AtCAD4_AAP59434.1	-----	340
AtCAD5_AAP59435.1	-----	340
CsCAD2_ADO51749.1	-----	340
FaCAD_AAK28509.1	-----	340
CADsc6s_PRUPE_pp=007622m	-----	340
CADsc8s_PRUPE_pp=007736m	-----	340
EjCAD1_ABV44810.1	-----	340
PmCAD_BAE48658.1	-----	340
AtCAD4_AAP59434.1	-----	340
AtCAD5_AAP59435.1	-----	340
CsCAD2_ADO51749.1	-----	340
FaCAD_AAK28509.1	-----	340
CADsc6s_PRUPE_pp=007622m	-----	340
CADsc8s_PRUPE_pp=007736m	-----	340
EjCAD1_ABV44810.1	-----	340
PmCAD_BAE48658.1	-----	340
AtCAD4_AAP59434.1	-----	340
AtCAD5_AAP59435.1	-----	340
CsCAD2_ADO51749.1	-----	340
FaCAD_AAK28509.1	-----	340
CADsc6s_PRUPE_pp=007622m	-----	340
CADsc8s_PRUPE_pp=007736m	-----	340
EjCAD1_ABV44810.1	-----	340
PmCAD_BAE48658.1	-----	340
AtCAD4_AAP59434.1	-----	340
AtCAD5_AAP59435.1	-----	340
CsCAD2_ADO51749.1	-----	340
FaCAD_AAK28509.1	-----	340
CADsc6s_PRUPE_pp=007622m	-----	340
CADsc8s_PRUPE_pp=007736m	-----	340
EjCAD1_ABV44810.1	-----	340
PmCAD_BAE48658.1	-----	340</

